NAVAL POSTGRADUATE SCHOOL

MONTEREY, CALIFORNIA

THESIS

DESIGNING A SENSORLESS TORQUE ESTIMATOR FOR DIRECT TORQUE CONTROL OF AN INDUCTION MOTOR

by

Athanasios Tsoutsas

September 2009

Thesis Advisor:	Alexander L. Julian
Second Readers:	Roberto Cristi
	Xiaoping Yun

Approved for public release; distribution is unlimited

THIS PAGE INTENTIONALLY LEFT BLANK

REPORT DOCUMENTATION PAGE		Form Approved OMB No. 0704-0188

Public reporting burden for this collection of information is estimated to average 1 hour per response, including the time for reviewing instruction, searching existing data sources, gathering and maintaining the data needed, and completing and reviewing the collection of information. Send comments regarding this burden estimate or any other aspect of this collection of information, including suggestions for reducing this burden, to Washington headquarters Services, Directorate for Information Operations and Reports, 1215 Jefferson Davis Highway, Suite 1204, Arlington, VA 22202-4302, and to the Office of Management and Budget, Paperwork Reduction Project (0704-0188) Washington DC 20503.

1. AGENCY USE ONLY *(Leave blank)*	**2. REPORT DATE** September 2009	**3. REPORT TYPE AND DATES COVERED** Engineer's Thesis

4. TITLE AND SUBTITLE Designing a Sensorless Torque Estimator for Direct Torque Control of an Induction Motor	**5. FUNDING NUMBERS**
6. AUTHOR(S) Athanasios Tsoutsas	
7. PERFORMING ORGANIZATION NAME(S) AND ADDRESS(ES) Naval Postgraduate School Monterey, CA 93943-5000	**8. PERFORMING ORGANIZATION REPORT NUMBER**
9. SPONSORING /MONITORING AGENCY NAME(S) AND ADDRESS(ES) N/A	**10. SPONSORING/MONITORING AGENCY REPORT NUMBER**

11. SUPPLEMENTARY NOTES The views expressed in this thesis are those of the author and do not reflect the official policy or position of the Department of Defense or the U.S. Government.

12a. DISTRIBUTION / AVAILABILITY STATEMENT Approved for public release; distribution is unlimited	**12b. DISTRIBUTION CODE**

13. ABSTRACT (maximum 200 words)

Nowadays, transportation is a major cause of air pollution. Electric propulsion could replace the internal combustion engines of automobiles and reduce the emission of exhaust gases. The propulsion of an electric vehicle requires the design of an accurate electromagnetic torque estimator and an efficient control system in order to control the speed of the vehicle. This concept is conveyed through this thesis. An electromagnetic torque calculator of an induction motor is designed in the Simulink/Matlab environment through XILINX block sets. The accuracy of the torque estimator is verified using the Field Programmable Gate Array (FPGA). Furthermore, using the proper hardware and software, realistic conclusions about the performance of the electromagnetic torque estimator are drawn.

14. SUBJECT TERMS Induction Motor, Electromagnetic Torque Estimator, Field Programmable Gate Array (FPGA), XILINX.	**15. NUMBER OF PAGES** 87
	16. PRICE CODE

17. SECURITY CLASSIFICATION OF REPORT	**18. SECURITY CLASSIFICATION OF THIS PAGE**	**19. SECURITY CLASSIFICATION OF ABSTRACT**	**20. LIMITATION OF ABSTRACT**
Unclassified	Unclassified	Unclassified	UU

NSN 7540-01-280-5500 Standard Form 298 (Rev. 2-89)
Prescribed by ANSI Std. 239-18

THIS PAGE INTENTIONALLY LEFT BLANK

Approved for public release; distribution is unlimited

DESIGNING A SENSORLESS TORQUE ESTIMATOR FOR A DIRECT TORQUE CONTROL OF AN INDUCTION MOTOR

Athanasios Tsoutsas
Lieutenant, Hellenic Navy
B.S, Hellenic Naval Academy, 1999

Submitted in partial fulfillment of the
requirements for the degrees of

ELECTRICAL ENGINEER

and

MASTER OF SCIENCE IN ELECTRICAL ENGINEERING

from the

NAVAL POSTGRADUATE SCHOOL
September 2009

Author: Athanasios Tsoutsas

Approved by: Alexander L. Julian
Thesis Advisor

Roberto Cristi
Second Reader

Xiaoping Yun
Second Reader

Jeffrey B. Knorr
Chairman, Department of Electrical and Computer Engineering

THIS PAGE INTENTIONALLY LEFT BLANK

ABSTRACT

Nowadays, transportation is a major cause of air pollution. Electric propulsion could replace the internal combustion engines of automobiles and reduce the emission of exhaust gases. The propulsion of an electric vehicle requires the design of an accurate electromagnetic torque estimator and an efficient control system in order to control the speed of the vehicle. This concept is conveyed through this thesis. An electromagnetic torque calculator of an induction motor is designed in the Simulink/Matlab environment through XILINX block sets. The accuracy of the torque estimator is verified using the Field Programmable Gate Array (FPGA). Furthermore, using the proper hardware and software, realistic conclusions about the performance of the electromagnetic torque estimator are drawn.

THIS PAGE INTENTIONALLY LEFT BLANK

TABLE OF CONTENTS

THIS PAGE INTENTIONALLY LEFT BLANK

LIST OF FIGURES

LIST OF TABLES

THIS PAGE INTENTIONALLY LEFT BLANK

LIST OF ABREVIATIONS AND ACRONYMS

FPGA:	Field Programmable Gate Array
VHDL:	VHSIC Hardware Description Language
VHSIC:	Very High Speed Integrated Circuit
DC:	Direct Current

THIS PAGE INTENTIONALLY LEFT BLANK

ACKNOWLEDGMENTS

I would like to thank Professor Alex Julian for his guidance and teaching during this project.

THIS PAGE INTENTIONALLY LEFT BLANK

EXECUTIVE SUMMARY

Induction motors are used worldwide in many residential, commercial, industrial and utility applications. Recently, they are the preferred choice among the industrial motors due to the modern power electronics that improve their speed control. Vitally important for the speed control of a motor is the accurate estimation of the magnetic flux and the electromagnetic torque. Knowing the electromagnetic torque of a motor, we are able to control it and thus monitor the speed faster and more stably.

The purpose of this study is to design an electromagnetic torque estimator of a three-phase induction motor, without the use of any sensor. This goal is being achieved by building the mathematical model of the induction motor as well as deriving the electromagnetic torque equation by means of the proper transformations and mathematical tools. The analysis of the designed estimator is done through Simulink/Matlab, where the transient and steady state torque of the motor is determined. Furthermore, the experimental test of the estimator, using a real motor, power electronics and the Field Programmable Gate Array, proves its efficiency.

The electromagnetic torque equation of the motor in the arbitrary (qd0) reference frame becomes:

$$T_e = \frac{P}{2}\frac{3}{2}\left(i_{qs}\lambda_{ds} - i_{ds}\lambda_{qs}\right) \quad \text{(a)}$$

In the equation above:

- P stands for the number of the motor poles.
- The quantities i_{qs} and i_{ds} stand for the q-axis and d-axis currents respectfully.
- λ_{qs} and λ_{ds} stand for the magnetic fluxes on the q-axis and d-axis.

Equation (a) can be transformed into the stationary reference frame where the speed ($\omega = \frac{d\theta}{dt}$) is zero as:

$$T_e = \frac{P}{2}\frac{3}{2}\left(i^{qs}\lambda^{ds} - i^{ds}\lambda^{qs}\right) = \frac{P}{2}\frac{3}{2}\left\{i^{qs}\left(\int (v^{ds} - r_s i^{ds})dt\right) - i^{ds}\left(\int (v^{qs} - r_s i^{qs})dt\right)\right\} \quad \text{(b)}$$

The torque equation (b) depends on the transformed stator voltages (v^{qs} and v^{ds}), the stator currents (i^{qs} and i^{ds}) and the resistance of stator phases. Accordingly, the formulation of the torque equation is based on equation (b), and in the Simulink/Matlab environment, it can be designed as shown in Figure 1:

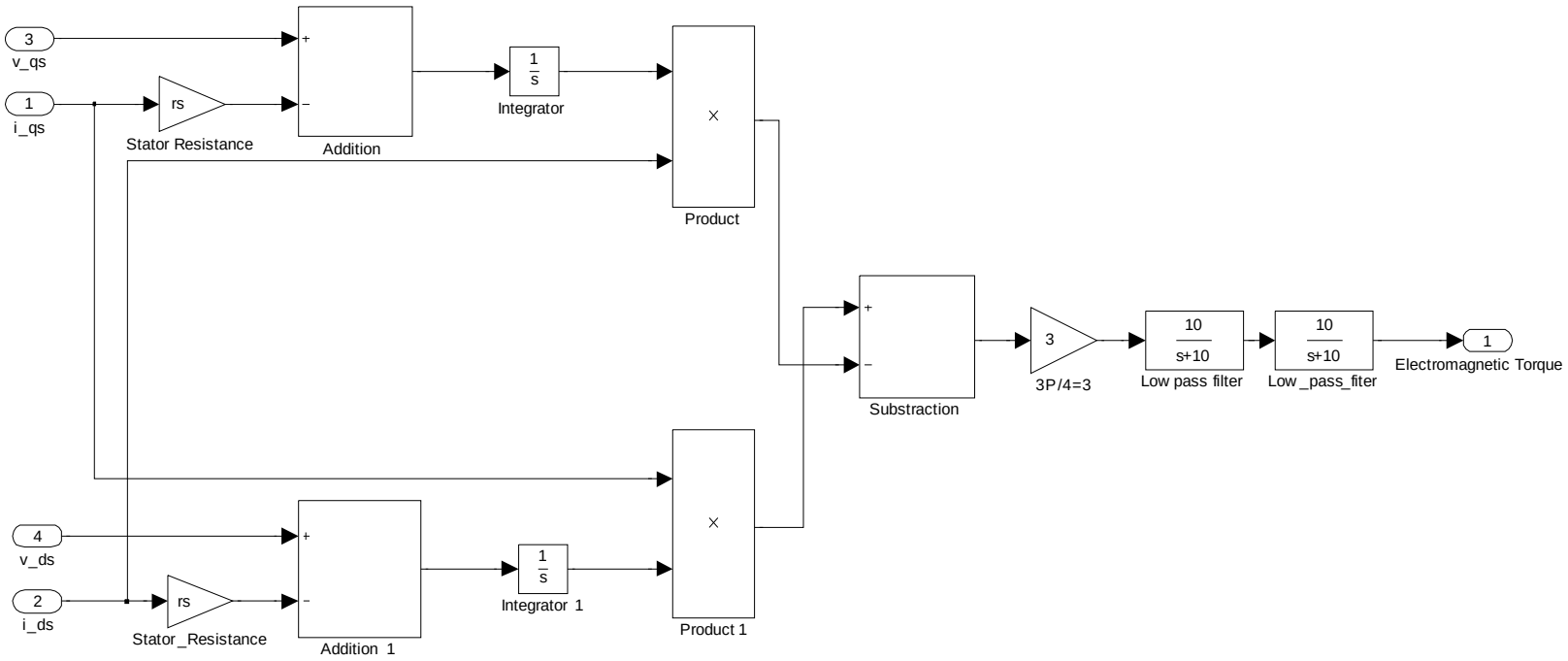

Figure 1. Torque Estimator in Simulink/Maltab Environment

The computation of the linkage fluxes $\left(\lambda^{qs}\right)$and $\left(\lambda^{ds}\right)$is achieved by means of the integration of the quantities $\left(v^{qs}-r_s i^{qs}\right)and\left(v^{ds}-r_s i^{ds}\right)$, respectively. An accurate integration of a waveform requires the exact determination of the initial conditions. These initial conditions should be determined in the block of integration. Otherwise, a constant value is added to the output waveform of the integration and the computed torque waveform has big ripples. The desired initial conditions of the magnetic flux are

not easily computed. Nevertheless, the two cascaded, first order, low pass filters at the output of the estimator eliminate the ripples and improve the integration procedure.

The final step of any design is the establishment of its quality, as well as the performance and the reliability of it. The experimental test is a procedure able to check whether the above criteria are satisfied. Using the state-of-the-art hardware and software developed in the power electronics laboratory at the Naval Postgraduate School, realistic conclusions about the performance of the electromagnetic torque estimator can be drawn. A schematic description of the laboratory experiment is demonstrated in Figure 2.

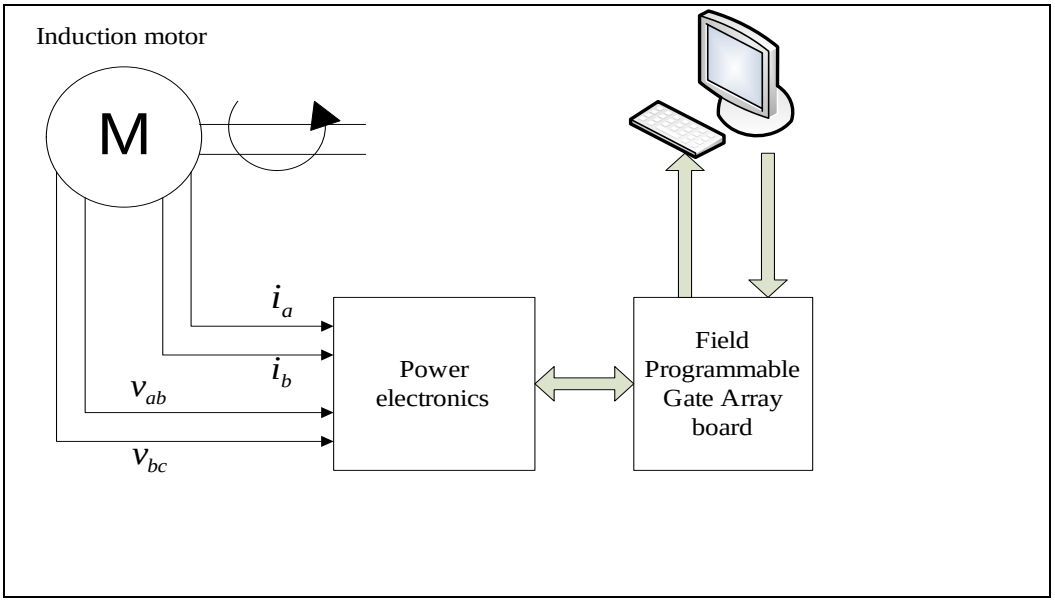

Figure 2. Schematic Description of the Laboratory Experiment

The induction motor is connected through the proper power electronics with the Field Programmable Gate Array. The electromagnetic torque estimator model is converted into XILINX blocks using the XILINX library contained in the Simulink/Matlab library browser. By means of the appropriate XILINX software, the Field Programmable Gate Array is programmed to execute the transformation of the signals into the stationary reference frame as well as the electromagnetic torque calculation. Consequently, as the induction motor accelerates or decelerates, the FPGA calculates the electromagnetic torque continuously. The results are plotted and analyzed on the computer.

The experimental application poses certain problems caused by the external noise interference and the appearance of constant offsets at the waveforms. The main problem, though, is related to the numerical integration. The flux is estimated through the integration of the stationary voltage and the current waveforms. However, if there is an offset at the input of the integrator, then a ramp error occurs at the output of the integration. The application of the operator ($1/(s+1)$) instead of the operator ($1/s$) gives a stable integration output. The flux integrator in XILINX software is thus going to be implemented as ($1/(s+1)$). Furthermore, the operator $1/(s+1)$ is transformed into the digital domain using the Euler approximation ($s = \frac{1-z^{-1}}{T_s}$) and it is implemented with elementary operations such as the time delay, the sum and the scaling.

The electromagnetic torque estimator in XILINX environment is shown in Figure 3:

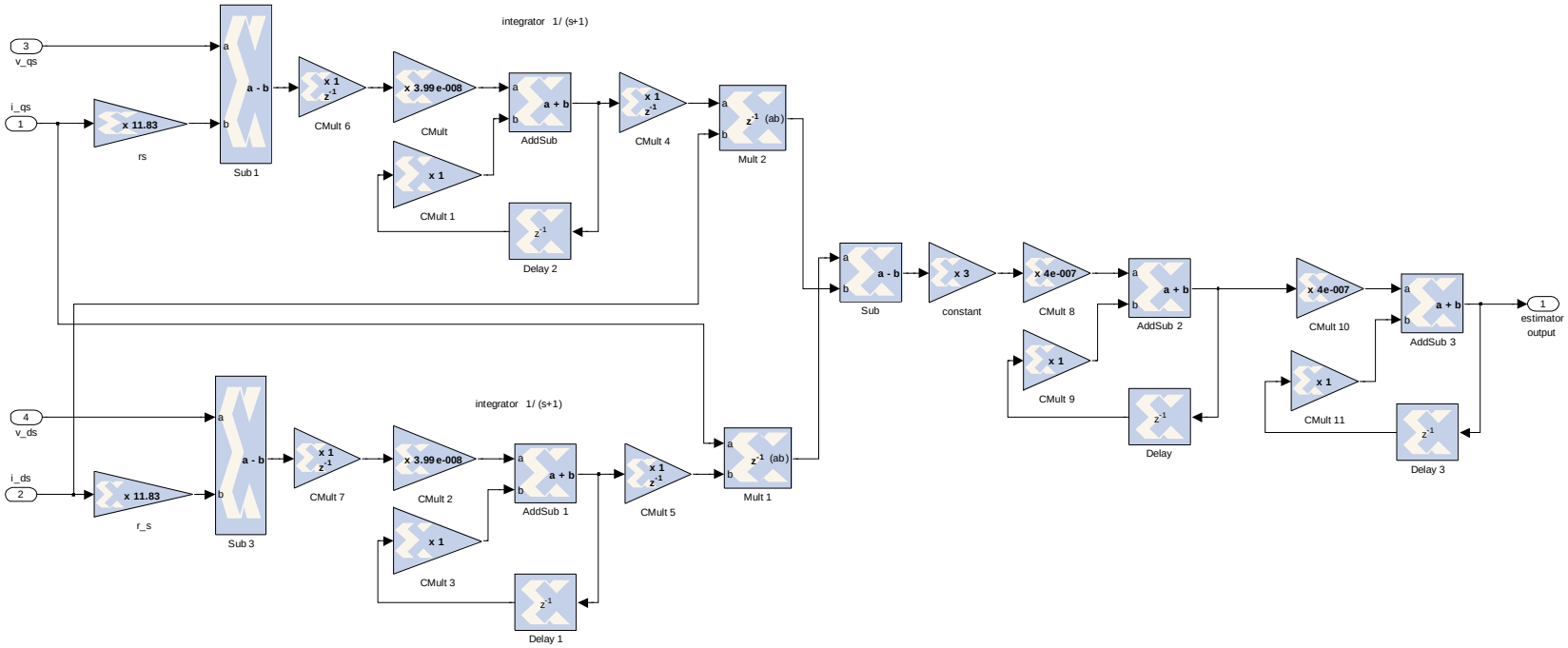

Figure 3. Torque Estimator in XILINX Environment

The accuracy of the electromagnetic torque estimator is verified by an electrodynamometer. The electrodynamometer is connected to the motor through a belt. It applies a mechanical torque to the motor, which, in ideal conditions, is equal to the electromagnetic torque. In practice, the measured electromagnetic torque should be a little bit larger in order to surpass the mechanical load and the losses. Since the difference is insignificant, though, the electrodynamometer is a good way to test the electromagnetic

torque estimator. A zero load condition has an initial electromagnetic torque of ($2.4\,lbf\,.in$). This value must certainly be added to the applied mechanical load. The final value deriving from this addition should thus be compared with the estimator measurement.

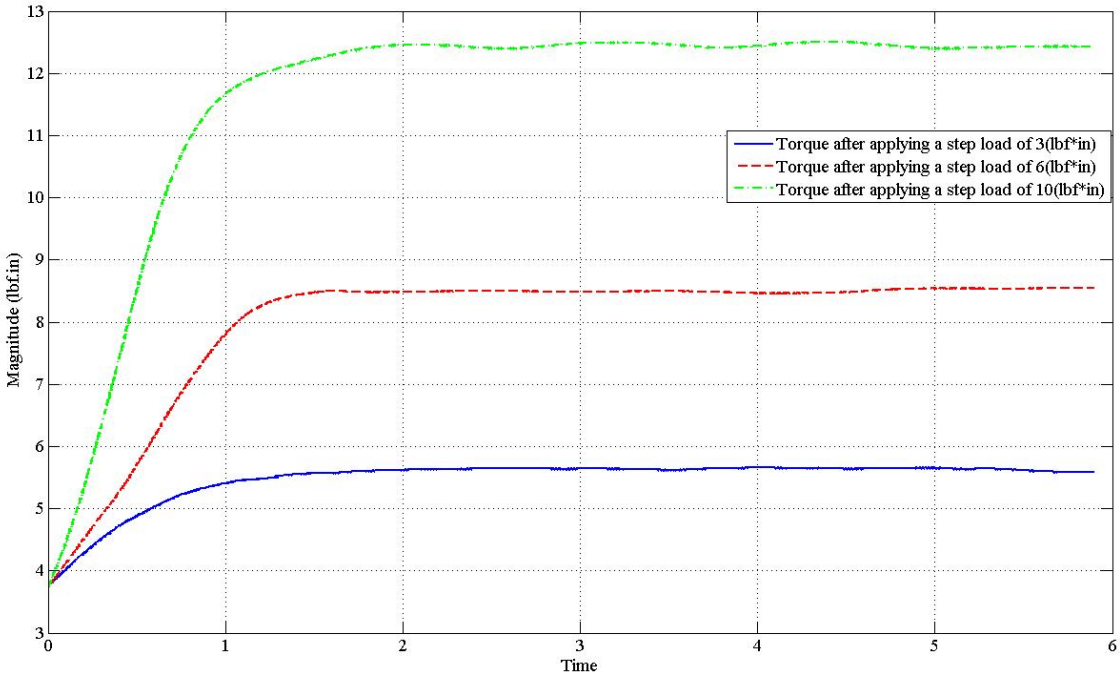

Figure 4. Electromagnetic Torque Response after Applying Three Different Step Loads

Three different step loads are applied at the motor, as seen in Figure 4. The calculated steady state torque approximates the electrodynamometer settings. The analysis of the results shows that the torque estimator works successfully for the induction motor.

THIS PAGE INTENTIONALLY LEFT BLANK

I. INTRODUCTION

A. BACKGROUND

Induction machines are used worldwide in many residential, commercial, industrial and utility applications. They transform electrical energy into mechanical energy. An induction motor may be part of a pump or fan, or connected to some other form of mechanical equipment such as a winder, a conveyor belt or a mixer. Induction motors have existed for many years but were always limited in their application because it was difficult to control the speed of the motor. Nowadays induction motors are the preferred choice among the industrial motors due to their rugged construction, the absence of brushes (which are required in most DC motors), the modern power electronics, and the ability to control the speed of the motor.

B. OBJECTIVE

There are certain kinds of applications that require the design of a very efficient estimator of the induction motor electromagnetic torque. An application of this kind is the electric vehicle. Knowing the electromagnetic torque we are able to control it. Furthermore, we can control the speed of the vehicle faster and more stably after adding a torque regulator to the speed loop. The accelerator of the electric vehicle could be a closed loop speed control system that would compute the electromagnetic torque, and would accordingly use that computation in order to control the torque and thus accelerate and decelerate the vehicle.

The objective of this study is to design an accurate electromagnetic torque estimator of a three-phase induction motor, without the use of any sensor. The designed torque estimator without any sensor is based on the mathematical model of the motor. It can easily be used to any control scheme without any influence on the efficiency of the motor.

C. INDUCTION MOTOR OVERVIEW

An induction motor is an electric motor that is driven by an alternating current. It consists of two basic parts: an outside stator having windings supplied with alternating current to produce the rotating magnetic field, and an inside rotor attached to the output shaft, as shown in Figure 5.

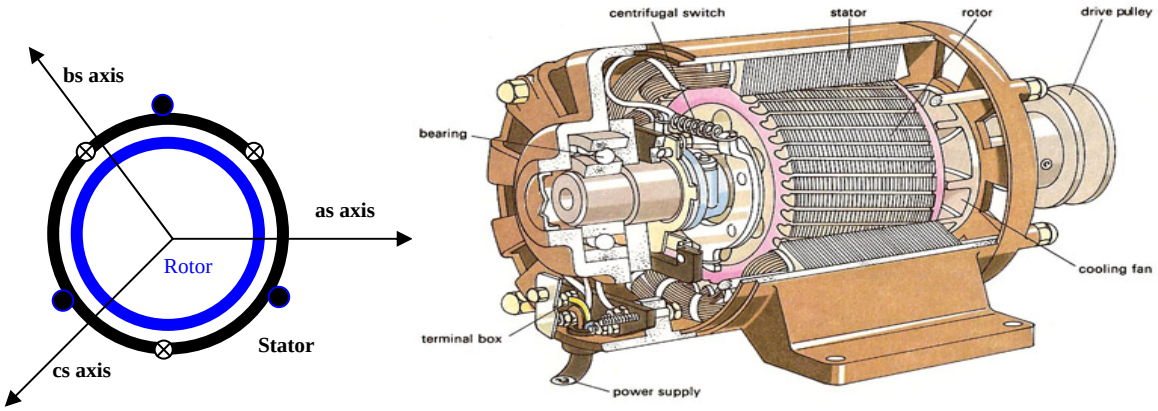

Figure 5. A Three-phase, wye-connected Induction Motor Schematic and a Real Induction Motor

There are two types of induction machine rotors: squirrel cage rotors and wound rotors. In this application a three-phases, four poles squirrel cage rotor induction motor is going to be used. In this kind of rotor the current flows through copper or aluminum bars. The bars, which are uniformly distributed and embedded in a ferromagnetic material, all end up at a common ring at each end of the rotor, as shown in Figure 6. This rotor structure is very simple, robust and reliable.

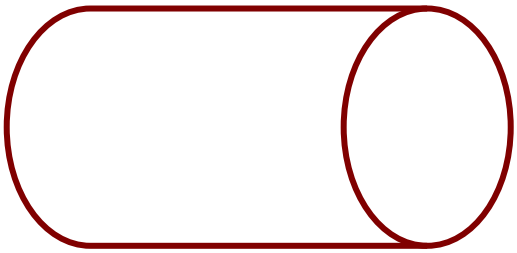

Figure 6. Squirrel Cage Rotor

As a consequence of the common ring existence at each end of the rotor, these aluminum conductors are short circuited. The current can thus flow up and down these aluminum bars. The operating principle of the induction motor is based on these currents. The stator windings create a rotating magnetic field. This changing magnetic field causes flux through these short-circuited loops of the rotor and induces current. The induced currents create another magnetic field that interacts with the magnetic field created by the stator and in effect causes a rotational motion in the rotor [1].

As a result of this operating principle the rotor cannot rotate at the same speed as the stator rotating field. If that happens, there will be neither change in the flux nor induced voltage, and consequently no induced currents in the rotor. Therefore, there will not be any reaction force against the stator rotating magnet motive force. Consequently, the rotor must always rotate more slowly than the stator rotating field, namely "slip." The question of how fast the rotor slips depends on the balance between the electromagnetic torque of the motor and the torque load [2].

D. APPROACH

An accurate estimator of the electromagnetic torque of a three-phase symmetrical induction motor is going to be designed without the use of any sensor. This goal is going to be achieved by building the mathematical model of the induction motor and deriving the appropriate mathematical equations that describe it. Using the proper transformations to reduce the complexity of these differential equations, the electromagnetic torque equation of the induction motor is going to be derived. The designed estimator, using Simulink/Matlab, will be based on that equation. The computer simulation will determine the transient and steady state torque of the motor. Furthermore, the computation of the torque of the real motor and the proof of the efficiency of our estimator will be done by converting the model in XILINX environment and using the XILINX FPGA (Field Programmable Gate Array).

The thesis is organized as follows. After the introduction of Chapter I, Chapter II contains the derivation of the torque equation, computer simulation and simulation

results. Chapter III describes the real implementation of the torque estimator and the hardware. Moreover, Chapter III analyzes the waveforms that have derived from the real application. Finally, Chapter IV includes general conclusions and possibilities for further research.

II. OBSERVER OF THE ELECTROMAGNETIC TORQUE

A. DERIVATION OF TORQUE EQUATION

1. Flux Linkage and Voltage Equations in the Arbitrary (qd0) Reference Frame

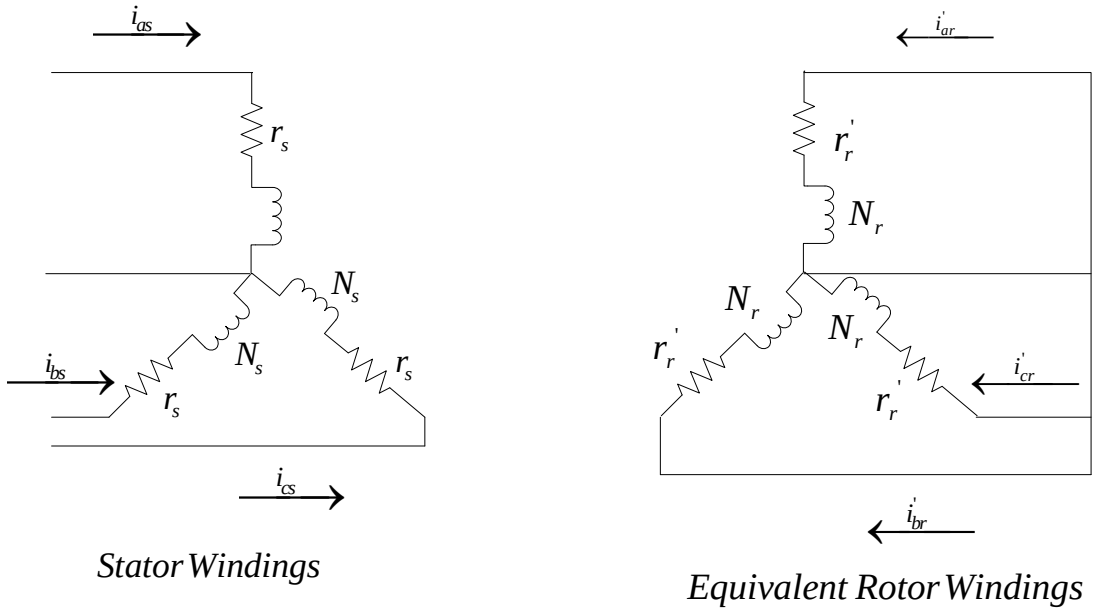

Figure 7. Circuitry Representation of the Squirrel Cage Induction Motor

A circuitry representation of the squirrel cage induction motor is shown in Figure 7. It is convenient for the analysis of the circuit to transform all rotor variables into the stator windings by appropriate turn ratios [1].

$$\left.\begin{aligned} i'_{abcr} &= \frac{N_r}{N_S} i_{abcr} \\ v'_{abcr} &= \frac{N_r}{N_S} v_{abcr} \\ \lambda'_{abcr} &= \frac{N_r}{N_S} \lambda_{abcr} \ (linkage\ flux) \\ r'_r &= \left(\frac{N_S}{N_r}\right)^2 r_r \end{aligned}\right\} \quad (1)$$

The voltage equations become:

$$\left.\begin{aligned} v_{as} &= r_s i_{as} + \frac{d\lambda_{as}}{dt} \\ v_{bs} &= r_s i_{bs} + \frac{d\lambda_{bs}}{dt} \\ v_{cs} &= r_s i_{cs} + \frac{d\lambda_{cs}}{dt} \end{aligned}\right\} \qquad (2)$$

$$\left.\begin{aligned} 0 &= r_r' i_{ar}' + \frac{d\lambda_{ar}'}{dt} \\ 0 &= r_r' i_{br}' + \frac{d\lambda_{br}'}{dt} \\ 0 &= r_r' i_{cr}' + \frac{d\lambda_{cr}'}{dt} \end{aligned}\right\} \qquad (3)$$

In our model, the total flux linking each of the three stator phases, as well as the rotor phases, is a combination of the six currents. Consequently, the flux linking each stator phase winding can be written as [1]:

$$\lambda_{as} = (L_{ls} + L_{ms})i_{as} + (-\frac{1}{2}L_{ms})i_{bs} + (-\frac{1}{2}L_{ms})i_{cs} + \left(\frac{N_s}{N_r}\right)L_{sr}\cos(\theta_r)i_{ar}' + \left(\frac{N_s}{N_r}\right)L_{sr}\cos(\theta_r + \frac{2\pi}{3})i_{br}' + \left(\frac{N_s}{N_r}\right)L_{sr}\cos(\theta_r - \frac{2\pi}{3})i_{cr}' \qquad (4)$$

$$\lambda_{bs} = (-\frac{1}{2}L_{ms})i_{as} + (L_{ls} + L_{ms})i_{bs} + (-\frac{1}{2}L_{ms})i_{cs} + \left(\frac{N_s}{N_r}\right)L_{sr}\cos(\theta_r - \frac{2\pi}{3})i_{ar}' + \left(\frac{N_s}{N_r}\right)L_{sr}\cos(\theta_r)i_{br}' + \left(\frac{N_s}{N_r}\right)L_{sr}\cos(\theta_r + \frac{2\pi}{3})i_{cr}' \qquad (5)$$

$$\lambda_{cs} = (-\frac{1}{2}L_{ms})i_{as} + (-\frac{1}{2}L_{ms})i_{bs} + (L_{ls} + L_{ms})i_{cs} + \left(\frac{N_s}{N_r}\right)L_{sr}\cos(\theta_r + \frac{2\pi}{3})i_{ar}' + \left(\frac{N_s}{N_r}\right)L_{sr}\cos(\theta_r - \frac{2\pi}{3})i_{br}' + \left(\frac{N_s}{N_r}\right)L_{sr}\cos(\theta_r)i_{cr}' \qquad (6)$$

$$\lambda_{ar}^{'} = \left(\frac{N_s}{N_r}\right) L_{sr}\cos(\theta_r) i_{as} + \left(\frac{N_s}{N_r}\right) L_{sr}\cos(\theta_r - \frac{2\pi}{3}) i_{bs} + \left(\frac{N_s}{N_r}\right) L_{sr}\cos(\theta_r + \frac{2\pi}{3}) i_{cs} + \left\{\left(\frac{N_s}{N_r}\right)^2 L_{lr} + L_{mr}\right\} i_{ar}^{'} + \left(-\frac{1}{2} L_{mr}\right) i_{br}^{'} + \left(-\frac{1}{2} L_{mr}\right) i_{cr}^{'} \qquad (7)$$

$$\lambda_{br}^{'} = \left(\frac{N_s}{N_r}\right) L_{sr}\cos(\theta_r + \frac{2\pi}{3}) i_{as} + \left(\frac{N_s}{N_r}\right) L_{sr}\cos(\theta_r) i_{bs} + \left(\frac{N_s}{N_r}\right) L_{sr}\cos(\theta_r - \frac{2\pi}{3}) i_{cs} + \left(-\frac{1}{2} L_{mr}\right) i_{ar}^{'} + \left\{\left(\frac{N_s}{N_r}\right)^2 L_{lr} + L_{mr}\right\} i_{br}^{'} + \left(-\frac{1}{2} L_{mr}\right) i_{cr}^{'} \qquad (8)$$

$$\lambda_{cr}^{'} = \left(\frac{N_s}{N_r}\right) L_{sr}\cos(\theta_r - \frac{2\pi}{3}) i_{as} + \left(\frac{N_s}{N_r}\right) L_{sr}\cos(\theta_r + \frac{2\pi}{3}) i_{bs} + \left(\frac{N_s}{N_r}\right) L_{sr}\cos(\theta_r) i_{cs} + \left(-\frac{1}{2} L_{mr}\right) i_{ar}^{'} + \left(-\frac{1}{2} L_{mr}\right) i_{br}^{'} + \left\{\left(\frac{N_s}{N_r}\right)^2 L_{lr} + L_{mr}\right\} i_{cr}^{'} \qquad (9)$$

In the above equations, L_{ls} and L_{ms} respectively stand for the leakage and magnetizing inductances of the stator windings; L_{lr} and L_{mr} are defined as the leakage and magnetizing inductances for the rotor windings, and the inductance L_{sr} is the amplitude of the mutual inductances between the stator and the rotor windings. The quantity θ_r is the electrical angular displacement of the rotor with respect to the (as) axis.

We can combine the flux linkages of the stator in a matrix form as follows:

$$\begin{bmatrix} \lambda_{as} \\ \lambda_{bs} \\ \lambda_{cs} \end{bmatrix} = L_s \begin{bmatrix} i_{as} \\ i_{bs} \\ i_{cs} \end{bmatrix} + L_{sr}^{'} \begin{bmatrix} i_{ar}^{'} \\ i_{br}^{'} \\ i_{cr}^{'} \end{bmatrix} \qquad (10)$$

The winding inductances in matrix form are [1]:

$$L_s = \begin{bmatrix} L_{ls} + L_{ms} & -\frac{1}{2}L_{ms} & -\frac{1}{2}L_{ms} \\ -\frac{1}{2}L_{ms} & L_{ls} + L_{ms} & -\frac{1}{2}L_{ms} \\ -\frac{1}{2}L_{ms} & -\frac{1}{2}L_{ms} & L_{ls} + L_{ms} \end{bmatrix} \qquad (11)$$

$$L_r = \begin{bmatrix} \left(\frac{N_s}{N_r}\right)^2 L_{lr} + L_{mr} & -\frac{1}{2}L_{mr} & -\frac{1}{2}L_{mr} \\ -\frac{1}{2}L_{mr} & \left(\frac{N_s}{N_r}\right)^2 L_{lr} + L_{mr} & -\frac{1}{2}L_{mr} \\ -\frac{1}{2}L_{mr} & -\frac{1}{2}L_{mr} & \left(\frac{N_s}{N_r}\right)^2 L_{lr} + L_{mr} \end{bmatrix} \qquad (12)$$

$$L_{rs}^{'} = \frac{N_s}{N_r} L_{sr} \begin{bmatrix} \cos\theta_r & \cos(\theta_r + \frac{2\pi}{3}) & \cos(\theta_r - \frac{2\pi}{3}) \\ \cos(\theta_r - \frac{2\pi}{3}) & \cos\theta_r & \cos(\theta_r + \frac{2\pi}{3}) \\ \cos(\theta_r + \frac{2\pi}{3}) & \cos(\theta_r - \frac{2\pi}{3}) & \cos\theta_r \end{bmatrix} \qquad (13)$$

The complexity of our mathematical analysis, which is required for the derivation of the electromagnetic torque equation, can be reduced by transforming the variables associated with the stator and the rotor elements into the arbitrary (qd0) reference frame. In general, the desired variables can be transformed into the arbitrary (qd0) reference frame by multiplying them by the proper transformation matrices.

The proper transformation matrices for the stationary and rotor variables are respectively [1]:

$$K_s = \frac{2}{3}\begin{bmatrix} \cos(\theta) & \cos(\theta-\frac{2\pi}{3}) & \cos(\theta+\frac{2\pi}{3}) \\ \sin(\theta) & \sin(\theta-\frac{2\pi}{3}) & \sin(\theta+\frac{2\pi}{3}) \\ \frac{1}{2} & \frac{1}{2} & \frac{1}{2} \end{bmatrix} \qquad (14)$$

$$K_r = \frac{2}{3}\begin{bmatrix} \cos(\theta-\theta_r) & \cos(\theta-\theta_r-\frac{2\pi}{3}) & \cos(\theta-\theta_r+\frac{2\pi}{3}) \\ \sin(\theta-\theta_r) & \sin(\theta-\theta_r-\frac{2\pi}{3}) & \sin(\theta-\theta_r+\frac{2\pi}{3}) \\ \frac{1}{2} & \frac{1}{2} & \frac{1}{2} \end{bmatrix} \qquad (15)$$

In the above transformation matrices θ is the angular displacement of the arbitrary reference frame.

A change of variables that formulates a transformation of variables of stationary circuit elements to the arbitrary reference frame can be expressed as:

$$\begin{bmatrix} f_{qs} \\ f_{ds} \\ f_{os} \end{bmatrix} = K_s \begin{bmatrix} f_{as} \\ f_{bs} \\ f_{cs} \end{bmatrix} \qquad (16)$$

where f is an arbitrary variable.

The following result is derived

$$\left.\begin{aligned} \lambda_{qs} &= L_{ls} i_{qs} + \frac{3}{2} L_{ms}\left(i_{qs} + i'_{qr}\right) \\ \lambda_{ds} &= L_{ls} i_{ds} + \frac{3}{2} L_{ms}\left(i_{ds} + i'_{dr}\right) \\ \lambda_{0s} &= L_{ls} i_{0s} \end{aligned}\right\} \qquad (17)$$

This can be seen from equation (10)

$$\begin{bmatrix}\lambda_{as}\\ \lambda_{bs}\\ \lambda_{cs}\end{bmatrix} = L_s\begin{bmatrix}i_{as}\\ i_{bs}\\ i_{cs}\end{bmatrix} + L_{sr}^{'}\begin{bmatrix}i_{ar}^{'}\\ i_{br}^{'}\\ i_{cr}^{'}\end{bmatrix}$$

Multiplying both sides by K_s and transforming the stator and rotor currents into the arbitrary reference frame using equation (16), it is obtained

$$K_s\begin{bmatrix}\lambda_{as}\\ \lambda_{bs}\\ \lambda_{cs}\end{bmatrix} = K_sL_sK_s^{-1}\begin{bmatrix}i_{qs}\\ i_{ds}\\ i_{0s}\end{bmatrix} + K_sL_{sr}^{'}K_r^{-1}\begin{bmatrix}i_{qr}^{'}\\ i_{dr}^{'}\\ i_{0r}^{'}\end{bmatrix}$$

The left hand side is the flux linkages of the stator in the arbitrary (qd0) reference frame in a matrix form. Knowing that $K_sL_sK_s^{-1}$ and $K_sL_{sr}^{'}K_r^{-1}$ are diagonal it is obtained [1]

$$\begin{bmatrix}\lambda_{qs}\\ \lambda_{ds}\\ \lambda_{0s}\end{bmatrix} = \begin{bmatrix}L_{ls}+\frac{3}{2}L_{ms} & 0 & 0\\ 0 & L_{ls}+\frac{3}{2}L_{ms} & 0\\ 0 & 0 & L_{ls}\end{bmatrix}\begin{bmatrix}i_{qs}\\ i_{ds}\\ i_{0s}\end{bmatrix} + \begin{bmatrix}\frac{3}{2}L_{ms} & 0 & 0\\ 0 & \frac{3}{2}L_{ms} & 0\\ 0 & 0 & 0\end{bmatrix}\begin{bmatrix}i_{qr}^{'}\\ i_{dr}^{'}\\ i_{0r}^{'}\end{bmatrix}$$

and equation (17) follows easily.

The determination of the stator voltage expressions in the arbitrary (qd0) reference frame is required for the derivation of the electromagnetic torque equation.

Equation (2) can be represented in a matrix form as follows

$$\begin{bmatrix}v_{as}\\ v_{bs}\\ v_{cs}\end{bmatrix} = \begin{bmatrix}r_s & 0 & 0\\ 0 & r_s & 0\\ 0 & 0 & r_s\end{bmatrix}\begin{bmatrix}i_{as}\\ i_{bs}\\ i_{cs}\end{bmatrix} + \frac{d}{dt}\begin{bmatrix}\lambda_{as}\\ \lambda_{bs}\\ \lambda_{cs}\end{bmatrix}$$

Multiplying both sides by K_s and transforming the stator currents and the linkage fluxes into the arbitrary (qd0) reference frame it is obtained:

$$K_s\begin{bmatrix} v_{as} \\ v_{bs} \\ v_{cs} \end{bmatrix} = K_s\begin{bmatrix} r_s & 0 & 0 \\ 0 & r_s & 0 \\ 0 & 0 & r_s \end{bmatrix}\left(K_s^{-1}\begin{bmatrix} i_{qs} \\ i_{ds} \\ i_{0s} \end{bmatrix}\right) + K_s\frac{d}{dt}\left(K_s^{-1}\begin{bmatrix} \lambda_{qs} \\ \lambda_{ds} \\ \lambda_{0s} \end{bmatrix}\right)$$

Computing the derivative at the right hand side, it is derived

$$K_s\begin{bmatrix} v_{as} \\ v_{bs} \\ v_{cs} \end{bmatrix} = K_sK_s^{-1}\begin{bmatrix} r_s & 0 & 0 \\ 0 & r_s & 0 \\ 0 & 0 & r_s \end{bmatrix}\begin{bmatrix} i_{qs} \\ i_{ds} \\ i_{0s} \end{bmatrix} + K_s\frac{d}{dt}\left(K_s^{-1}\right)\begin{bmatrix} \lambda_{qs} \\ \lambda_{ds} \\ \lambda_{0s} \end{bmatrix} + K_sK_s^{-1}\frac{d}{dt}\begin{bmatrix} \lambda_{qs} \\ \lambda_{ds} \\ \lambda_{0s} \end{bmatrix}$$

The left hand side represents the stator voltages in the arbitrary reference frame in a matrix form. Knowing that $K_sK_s^{-1}$ is the unity matrix and computing the term $K_s\frac{d}{dt}\left(K_s^{-1}\right)$ it is obtained

$$\begin{bmatrix} v_{qs} \\ v_{ds} \\ v_{0s} \end{bmatrix} = \begin{bmatrix} r_s & 0 & 0 \\ 0 & r_s & 0 \\ 0 & 0 & r_s \end{bmatrix}\begin{bmatrix} i_{qs} \\ i_{ds} \\ i_{0s} \end{bmatrix} + \frac{d\theta}{dt}\begin{bmatrix} 0 & 1 & 0 \\ -1 & 0 & 0 \\ 0 & 0 & 0 \end{bmatrix}\begin{bmatrix} \lambda_{qs} \\ \lambda_{ds} \\ \lambda_{0s} \end{bmatrix} + \frac{d}{dt}\begin{bmatrix} \lambda_{qs} \\ \lambda_{ds} \\ \lambda_{0s} \end{bmatrix}$$

and expanding the matrices it follows that the stator voltage equations in the arbitrary reference frame are

$$\left.\begin{aligned} v_{qs} &= r_s i_{qs} + \frac{d\theta}{dt}\lambda_{ds} + \frac{d}{dt}\left(\lambda_{qs}\right) \\ v_{ds} &= r_s i_{ds} - \frac{d\theta}{dt}\lambda_{qs} + \frac{d}{dt}\left(\lambda_{ds}\right) \\ v_{0s} &= r_s i_{qs} + \frac{d}{dt}\left(\lambda_{0s}\right) \end{aligned}\right\} \qquad (18)$$

2. Electromagnetic Torque Equation

The total energy stored in a rotating electromagnetic system with J electrical inputs can be expressed as [1]:

$$W_f(i_1, i_2, ..., \theta_r) = \frac{1}{2}\sum_{p=1}^{J}\sum_{q=1}^{J} L_{pq} i_p i_q \qquad (19)$$

In the case of the three-phase induction motor, there exist two electrical inputs; the stator and the rotor. Equation (19) is reduced as [1]:

$$W_f(i_1, i_2, \theta_r) = \frac{1}{2} L_{11} i_1^2 + L_{12} i_1 i_2 + \frac{1}{2} L_{22} i_2^2 \qquad (20)$$

The term L_{11} describes the partial derivative of the linkage flux of the first input with respect to the current of the first input ($\frac{\partial \lambda_1(i_1, i_2, \theta_r)}{\partial i_1}$), while L_{12} describes the partial derivative of the flux of the first input with respect to the current of the second input ($\frac{\partial \lambda_1(i_1, i_2, \theta_r)}{\partial i_2}$), and finally L_{22} stands for the derivative of the flux of the second input with respect to the current of that ($\frac{\partial \lambda_2(i_1, i_2, \theta_r)}{\partial i_2}$). The energy stored in the (a) phase of the motor only is derived by combining the equations (4), (7) and (20):

$$W_f(i_{as}, i_{ar}^{'}, \theta_r) = \frac{1}{2}(L_{ls} + L_{ms}) i_{as}^2 + \left(\frac{N_s}{N_r}\right) L_{sr} \cos(\theta_r) i_{as} i_{ar}^{'} + \frac{1}{2}\left\{\left(\frac{N_s}{N_r}\right)^2 L_{lr} + L_{mr}\right\} i_{ar}^{'\,2}$$

Following the same procedure through all three phases of the induction motor, the total energy stored in the coupling fields can be written as:

$$W_f = \frac{1}{2} L_s \left(i_{as}^2 + i_{bs}^2 + i_{cs}^2\right) + \begin{bmatrix} i_{as} & i_{bs} & i_{cs} \end{bmatrix} L_{sr}^{'} \begin{bmatrix} i_{ar}^{'} \\ i_{br}^{'} \\ i_{cr}^{'} \end{bmatrix} + \frac{1}{2} L_r^{'} \left(i_{ar}^{'\,2} + i_{br}^{'\,2} + i_{cr}^{'\,2}\right) \qquad (21)$$

In rotational systems, the electromagnetic torque is defined as the derivative of the co-energy W_c with respect to the actual angular displacement of the rotor θ_{rm}. Assuming that the motor is magnetically linear then the field energy is equal to the co-energy. Furthermore, the actual angular displacement of the rotor for a P-pole motor is related to the electric angular displacement as [1]:

$$\theta_r = \left(\frac{P}{2}\right)\theta_{rm} \qquad (22)$$

So, the electromagnetic torque may be expressed as [1]:

$$T_e(i_j,\theta_r) = \frac{\partial W_c(i_j,\theta_r)}{\partial \theta_{rm}} = \frac{P}{2}\frac{\partial W_f(i_j,\theta_r)}{\partial \theta_r}$$

using equation (20) to obtain

$$T_e(i_j,\theta_r) = \frac{P}{2}\frac{\partial}{\partial \theta_r}\left\{\frac{1}{2}L_s\left(i_{as}^2 + i_{bs}^2 + i_{cs}^2\right) + \begin{bmatrix} i_{as} & i_{bs} & i_{cs}\end{bmatrix} L_{sr}^{'}\begin{bmatrix} i_{ar}^{'} \\ i_{br}^{'} \\ i_{cr}^{'}\end{bmatrix} + \frac{1}{2}L_r^{'}\left(i_{ar}^{'\,2} + i_{br}^{'\,2} + i_{cr}^{'\,2}\right)\right\}$$

then, after simple substitutions it is obtained

$$T_e(i_j,\theta_r) = \cancel{\frac{P}{2}\frac{\partial}{\partial \theta_r}\left\{\frac{1}{2}L_s\left(i_{as}^2 + i_{bs}^2 + i_{cs}^2\right)\right\}} + \frac{P}{2}\frac{\partial}{\partial \theta_r}\left\{\begin{bmatrix} i_{as} & i_{bs} & i_{cs}\end{bmatrix} L_{sr}^{'}\begin{bmatrix} i_{ar}^{'} \\ i_{br}^{'} \\ i_{cr}^{'}\end{bmatrix}\right\} + \cancel{\frac{P}{2}\frac{\partial}{\partial \theta_r}\left\{\frac{1}{2}L_r^{'}\left(i_{ar}^{'\,2} + i_{br}^{'\,2} + i_{cr}^{'\,2}\right)\right\}}$$

and cancelling the derivatives that are equal to zero yields

$$T_e(i_j,\theta_r) = \frac{P}{2}\begin{bmatrix} i_{as} \\ i_{bs} \\ i_{cs}\end{bmatrix}^T \frac{\partial}{\partial \theta_r}\left(L_{sr}^{'}\right)\begin{bmatrix} i_{ar}^{'} \\ i_{br}^{'} \\ i_{cr}^{'}\end{bmatrix} \qquad (23)$$

Equation (23) can be transformed into the arbitrary reference frame as [1]:

$$T_e(i_j,\theta_r) = \frac{P}{2}\left(K_s^{-1}\begin{bmatrix} i_{qs} \\ i_{ds} \\ i_{0s}\end{bmatrix}\right)^T \frac{\partial}{\partial \theta_r}\left(L_{sr}^{'}\right)\left(K_r^{-1}\begin{bmatrix} i_{qr}^{'} \\ i_{dr}^{'} \\ i_{0r}^{'}\end{bmatrix}\right) = \frac{P}{2}\begin{bmatrix} i_{qs} \\ i_{ds} \\ i_{0s}\end{bmatrix}^T \left(K_s^{-1}\right)^T \frac{\partial}{\partial \theta_r}\left(L_{sr}^{'}\right)K_r^{-1}\begin{bmatrix} i_{qr}^{'} \\ i_{dr}^{'} \\ i_{0r}^{'}\end{bmatrix}$$

which yields

$$T_e = \frac{P}{2}\frac{6}{4}L_{ms}\left(i_{qs}i_{dr}^{'} - i_{ds}i_{qr}^{'}\right) \qquad (24)$$

Solving equation (17) to find $i_{qr}^{'}$ and $i_{dr}^{'}$ the following is derived:

$$i_{qr}^{'} = \frac{\lambda_{qs}}{\frac{3}{2}L_{ms}} - \left(\frac{L_{ls} + \frac{3}{2}L_{ms}}{\frac{3}{2}L_{ms}} \right) i_{qs} \qquad (25)$$

$$i_{dr}^{'} = \frac{\lambda_{ds}}{\frac{3}{2}L_{ms}} - \left(\frac{L_{ls} + \frac{3}{2}L_{ms}}{\frac{3}{2}L_{ms}} \right) i_{ds} \qquad (26)$$

Substituting equations (25) and (26) for equation (24), the final simple equation of the electromagnetic torque, which is a combination of the transformed stator currents and linkage fluxes, is derived:

$$T_e = \frac{P}{2}\frac{6}{4}L_{ms}\left(i_{qs}i_{dr}^{'} - i_{ds}i_{qr}^{'}\right) = \frac{P}{2}\frac{6}{4}L_{ms}\left\{ i_{qs}\frac{\lambda_{ds}}{\frac{3}{2}L_{ms}} - \cancel{\left(\frac{L_{ls} + \frac{3}{2}L_{ms}}{\frac{3}{2}L_{ms}} \right) i_{qs}i_{ds}} - i_{ds}\frac{\lambda_{qs}}{\frac{3}{2}L_{ms}} + \cancel{\left(\frac{L_{ls} + \frac{3}{2}L_{ms}}{\frac{3}{2}L_{ms}} \right) i_{ds}i_{qs}} \right\} =$$

$$\boxed{T_e = \frac{P}{2}\frac{3}{2}\left(i_{qs}\lambda_{ds} - i_{ds}\lambda_{qs}\right)} \qquad (27)$$

B. TORQUE ESTIMATOR IN SIMULINK/MATLAB ENVIROMENT.

1. Designing the Torque Estimator

Equation $T_e = \frac{P}{2}\frac{3}{2}\left(i_{qs}\lambda_{ds} - i_{ds}\lambda_{qs}\right)$ shows that the electromagnetic torque depends on the stator currents and the linkage fluxes. The stator currents are measurable quantities. There is electronic equipment that measures the current with great accuracy. On the other hand, the linkage flux is a quantity that is very difficult to be measured. This observation leads to the conclusion that the more accurate the estimation of the flux the more efficient the torque calculation. The design of an appropriate sensor, which could measure the flux and could be placed between the stator and the rotor, would solve the

problem. However, this idea, besides the constructional problems, could affect the magnetic fluxes in the motor and reduce its efficiency. On the other hand, torque estimation without any sensor, based on the mathematical model of the motor, could easily be used without any influence on the flux.

The analysis of the motor and the derivation of the voltage and magnetic flux equation have been done to the arbitrary reference frame. Nevertheless, a closer examination of voltage equations (18) shows that their transformation from the arbitrary into the stationary reference frame renders the desired linkage flux computation easier. The speed of the stationary reference frame is zero. In other words, the voltage equations are more easily solved by replacing ($\omega = \frac{d\theta}{dt}$) with zero. The q-axis and d-axis linkage fluxes in the stationary reference frame are respectively [5]:

$$\boxed{\lambda^{qs} = \int (v^{qs} - r_s i^{qs}) dt} \qquad (28)$$

$$\boxed{\lambda^{ds} = \int (v^{ds} - r_s i^{ds}) dt} \qquad (29)$$

which are derived by solving equations

$$v^{qs} = r_s i^{qs} + \cancel{\frac{d\theta}{dt}\lambda^{ds}} + \frac{d}{dt}\left(\lambda^{qs}\right) = r_s i^{qs} + \frac{d}{dt}\left(\lambda^{qs}\right)$$

$$v^{ds} = r_s i^{ds} - \cancel{\frac{d\theta}{dt}\lambda^{qs}} + \frac{d}{dt}\left(\lambda^{ds}\right) = r_s i^{ds} + \frac{d}{dt}\left(\lambda^{ds}\right)$$

after replacing ($\frac{d\theta}{dt} = 0$).

The torque equation in the stationary reference frame becomes:

$$T_e = \frac{P}{2}\frac{3}{2}\left(i^{qs}\lambda^{ds} - i^{ds}\lambda^{qs}\right) = \frac{P}{2}\frac{3}{2}\left\{i^{qs}\left(\int (v^{ds} - r_s i^{ds}) dt\right) - i^{ds}\left(\int (v^{qs} - r_s i^{qs}) dt\right)\right\} \qquad (30)$$

The final torque equation depends on the stator voltage, stator currents and the resistance of stator phases—quantities that can be measured accurately. Actually, the variation of the stator resistance with time/temperature is significant. The equations are very sensitive to the resistance, especially at low speed.

Accordingly, the torque estimator is formulated based on equation (30) and in the Simulink/Matlab environment it can be designed as in Figure 8:

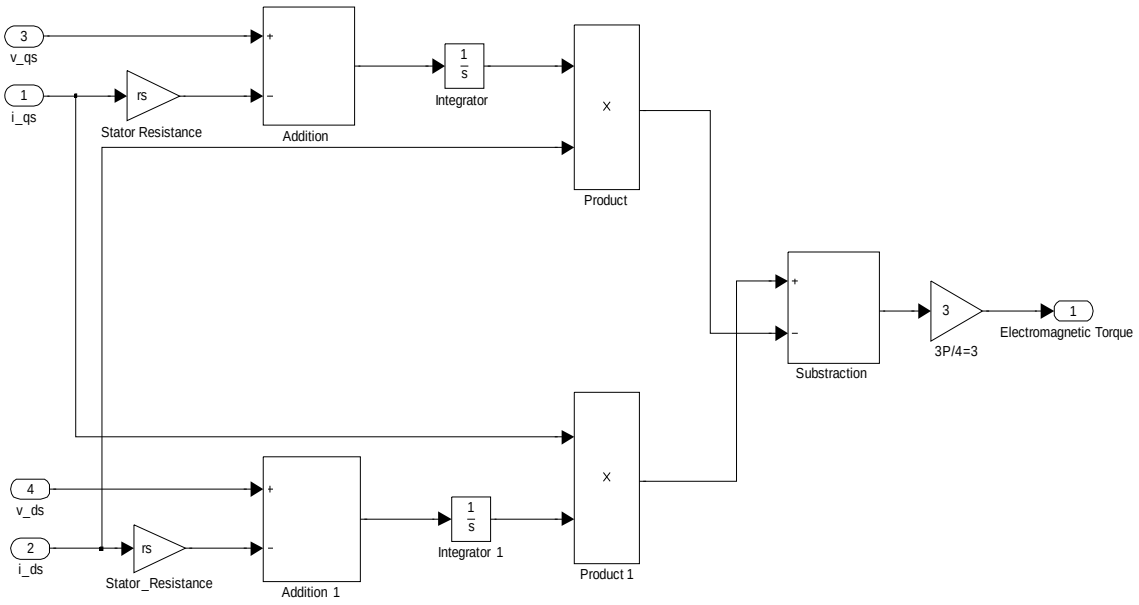

Figure 8. Torque Estimator in Simulink/Matlab Environment

Standard Simulink blocks are used for the implementation of this model. It consists of four inputs, the stator voltage and the stator currents in the stationary reference frame, and the desired electromagnetic torque as its output.

2. Computer Simulation—Analysis of the Results

A computer simulation model is going to be used in order to test the estimator. This model simulates a four pole, 60 Hz, three-phase induction motor with the following rating parameters:

Power	Phase voltage	rpm	r_s	$r_r^{'}$	L_{ls}	L_{ms}	$L_{lr}^{'}$
3 hp	220 Volts	1710	0.435 ohms	0.816 ohms	0.002 H	0.0462 H	0.002 H

Table 1. Parameters of the Computer Simulated Three-phase Induction Motor

The computer simulation model was designed in a way that allows us to choose the appropriate frequency speed and consequently to define the reference frame. Therefore, the four desired inputs to the estimator $\left(v_{qs}, v_{ds}, i_{qs}, i_{ds}\right)$, which are extracted from the computer model, are already transformed into the stationary reference frame [4].

The induction motor is simulated for a time (tstop = 2 sec) with the sample time of (tsample = 0.00002 sec). A step load torque is applied at (tstep = 0.5 sec) on the motor. Ideally, in the case of a motor driving a load, the load torque is equal to the electromagnetic torque. Consequently, the applied load torque affects the electromagnetic torque. The results are displayed and analyzed on a scope.

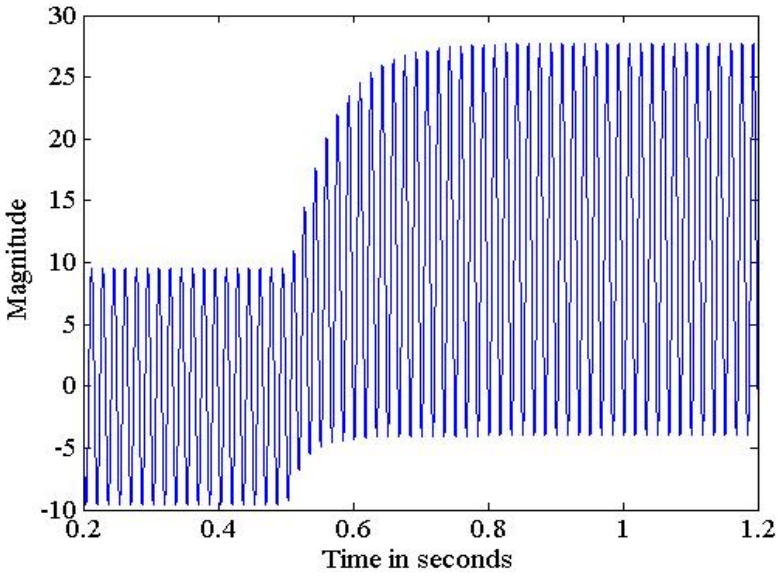

Figure 9. Electromagnetic Torque after Applying a Step Load Torque on the Motor

The output of the designed torque estimator, as shown in Figure 9, is not the expected output. After the application of the step function, in steady state, it should be constant without the ripples that appear in our case. Furthermore, in computer simulation the waveforms are perfect and, most importantly, they are not disturbed by the interference of any undesired external noise that could create these ripples.

The undesired ripples at the output are caused by the integration. The computation of the linkage fluxes $\left(\lambda^{qs}\right)$ and $\left(\lambda^{ds}\right)$ is achieved by the integration of the quantities $\left(v^{qs}-r_s i^{qs}\right)$ and $\left(v^{ds}-r_s i^{ds}\right)$ respectively. An accurate integration of a waveform requires the exact determination of the initial conditions.

Assuming that a sine waveform is integrated, it can be written [6]:

$$\int a\sin(\omega t)dt = -\frac{a}{\omega}\cos(\omega t) + \left(\underbrace{-\frac{a}{\omega}\cos(\omega t)\Big|_{t=0}}_{\text{Initial Conditions}} \right) \qquad (31)$$

These initial conditions should be determined in the block of integration. Otherwise, a constant value is added to the output waveform of the integration.

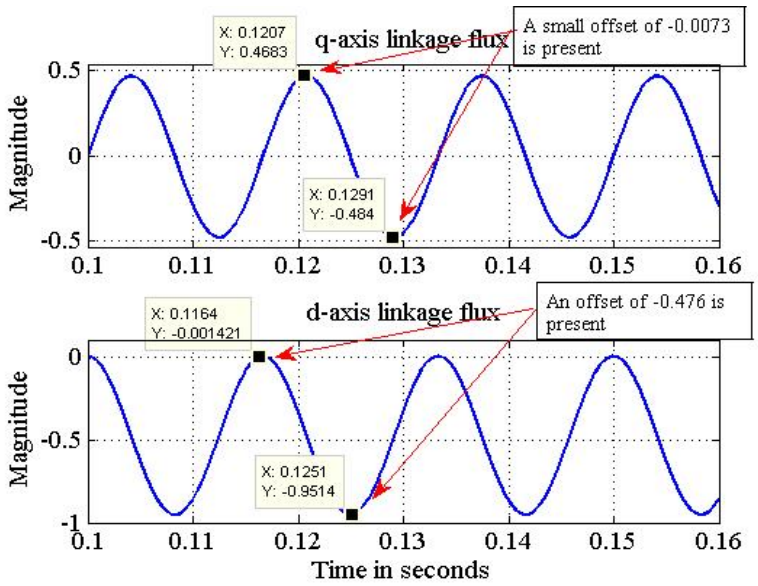

Figure 10. The Waveforms of the Linkage Fluxes Shifted Vertically by Constant Offsets

The subtraction of the two waveforms with offset causes the ripples that appear in the output torque of Figure 10. The desired initial conditions of the magnetic flux are not easily computed. Instead, there are two possible solutions against the integration problem.

a. Applying a High Pass Filter after the Integration

The application of a first order high pass filter before the integration blocks eliminates the offset values from the flux's waveforms and hence improves the integration procedure. The fundamental frequency of the waveforms is 60 Hz. So a high pass filter with a cutoff frequency of 10 Hz is selected as shown in Figure 11.

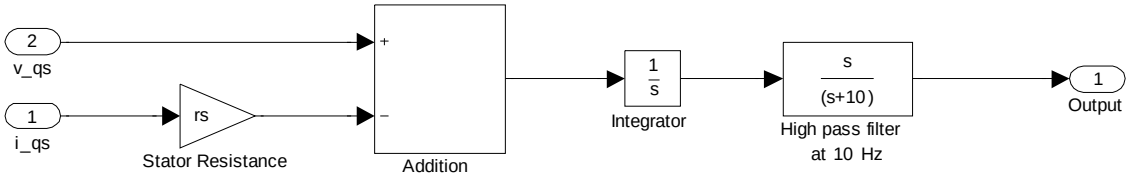

Figure 11. Applying a high pass filter after the integrator

The magnitude of the frequency response of a first order high pass filter with transfer function ($Tf = \frac{s}{s+10}$) can be displayed via a bode plot as shown in Figure 12.

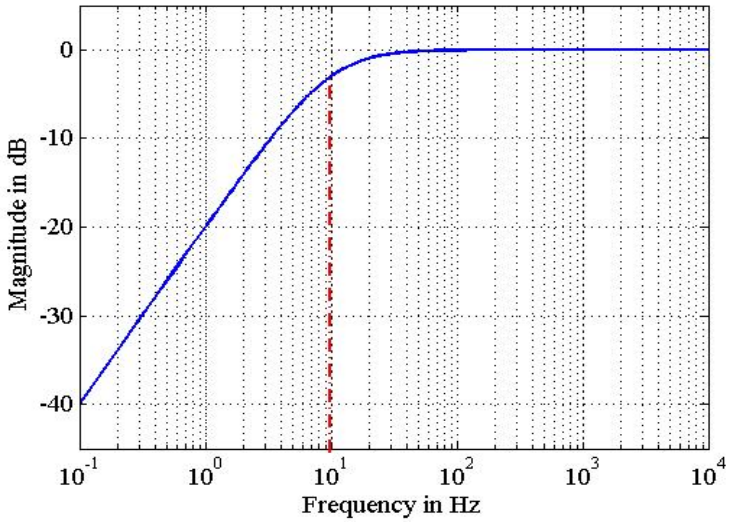

Figure 12. Frequency Response of a High Pass Filter with Transfer Function

$$Tf = s/s+10$$

The offset of the flux linkage waveforms has been removed by the high pass filters as shown in Figure 13.

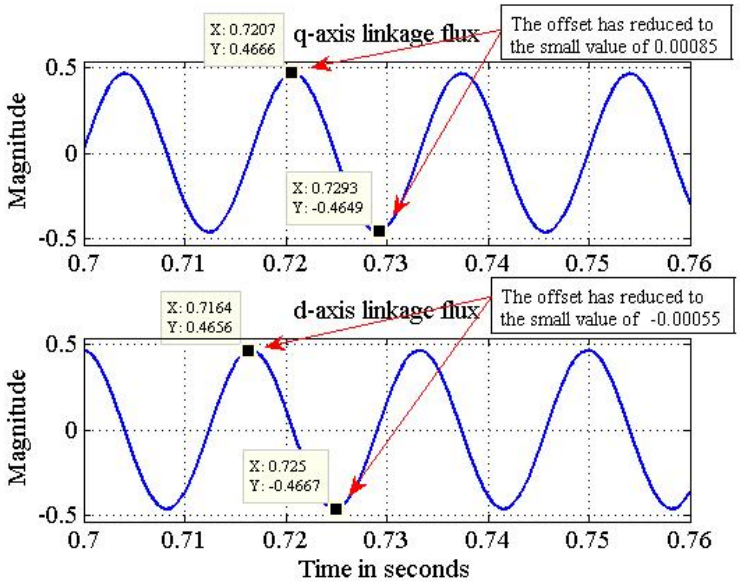

Figure 13. The Effect of the High Pass Filters on the Flux Linkage Waveforms in Steady State

After the adjustment, which has been made by the high pass filters, the electromagnetic torque is shown in Figure 14.

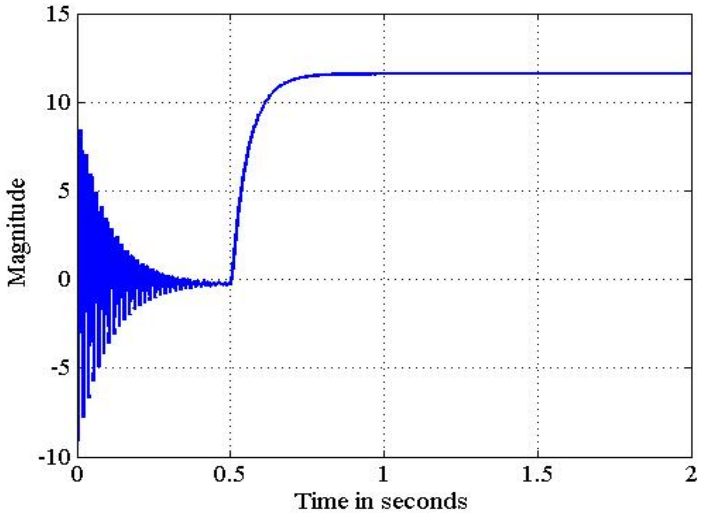

Figure 14. Electromagnetic Torque of the Motor after the Placement of Two High Pass Filters before the Integration Blocks on the Torque Estimator Model

b. Placing a Low Pass Filter in the Output of the Torque Estimator

The analysis of the undesired waveform of Figure 9 in the frequency domain can be made by computing the discrete Fourier transform of the signal. The discrete Fourier transform is an algorithm used in situations where there is not an analytical expression of a signal and hence its frequency spectrum needs to be determined. An efficient way of computing the discrete Fourier transform is the fast Fourier transform. By applying the fast Fourier transform on the signal of Figure 9, the spectrum in Figure 15 is obtained.

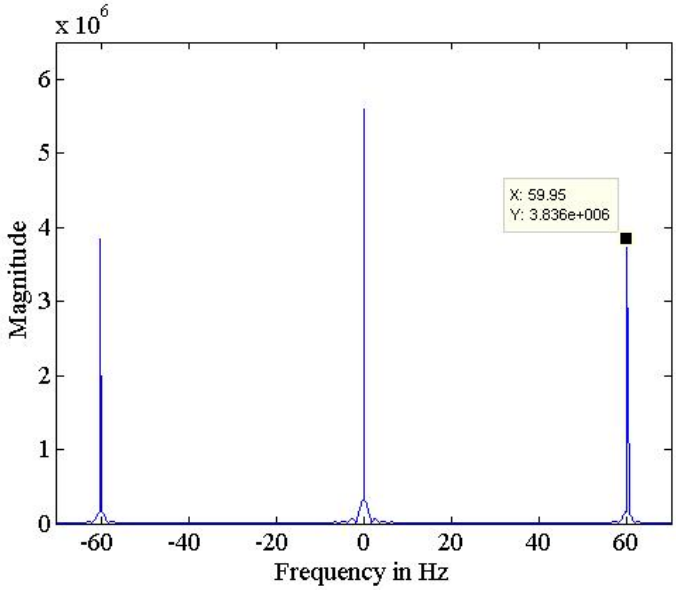

Figure 15. Fast Fourier Transform of the Signal Shown in Figure 9

The analysis of the frequency spectrum illustrated in Figure 15 shows that the signal contains a constant value quantity at 0 Hz and has a fundamental frequency of 60 Hz. In order to extract the constant quantity that in fact represents the electromagnetic torque, a low pass filter can be applied to the output of the torque estimator. As the fundamental frequency is at 60 Hz, a second order low pass filter with cutoff frequency of 10 Hz can be used to eliminate the unvarying quantity. The transfer function of the low pass filter can be:

$$Tf = \frac{100}{s^2 + 20s + 100}$$

The bode plot of the second order low pass filter is shown in Figure 16.

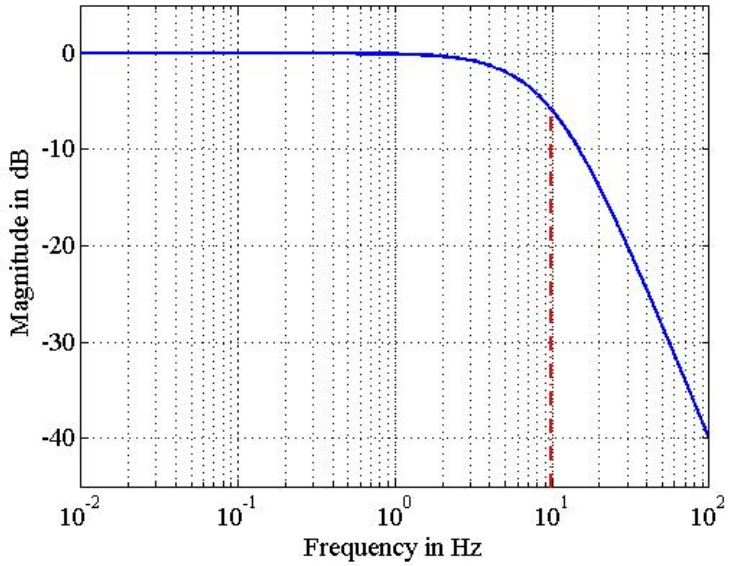

Figure 16. Frequency Response of a Second Order Filter with Transfer Function $Tf = 100/s^2 + 20s + 100$

The electromagnetic torque after the low pass filter becomes as shown in Figure 17.

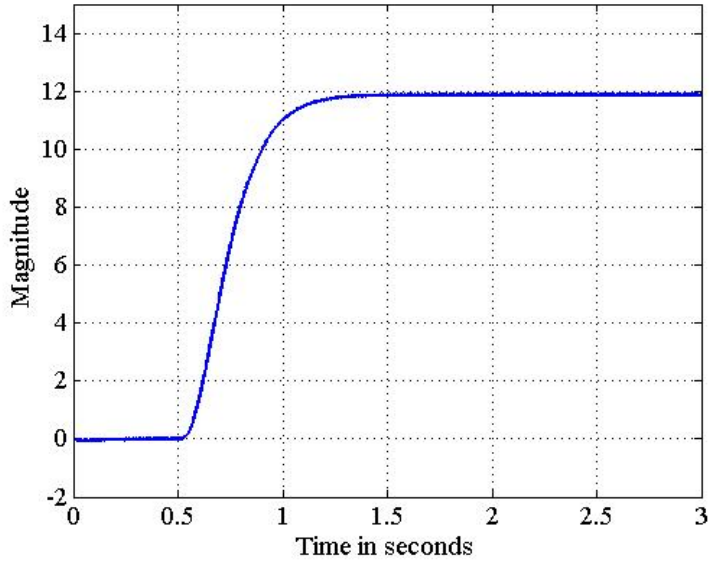

Figure 17. Electromagnetic Torque after Applying a Second Order Low Pass Filter to the Output of the Estimator

c. Comparing the Two Proposed Solutions

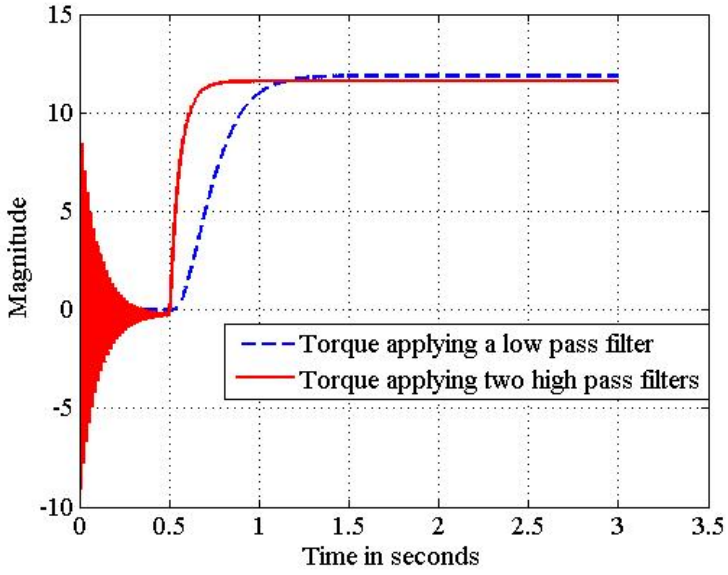

Figure 18. Comparing the Torque Diagrams after Applying a Low Pass Filter to the Output of the Estimator or Two High Pass Filters before the Integration Blocks

The implementation of two high pass filters affects the response of the electromagnetic torque as it reaches the steady state value faster, as seen in Figure 18. On the other hand, the steady state values are almost the same, proving that both solutions can be used with accurate steady state results. The implementation of the estimator in the computation of the electromagnetic torque of a real induction motor requires that it should be as simple as possible. It is easier to construct a low pass filter compared to a high pass filer. As a result, the final modification of the torque calculator is composed of an extra second order low pass filter at the end of it. The accuracy of the designed estimator is analyzed in the next chapter. Using the appropriate hardware and software, the torque of a real three-phase induction motor is computed continuously as the motor runs, giving an estimation of the precision of our torque calculator.

III. COMPUTING THE TORQUE OF A REAL MOTOR

A. HARDWARE DESCRIPTION

The final step of any design is the establishment of its quality, and the performance and the reliability of it. The experimental test is a procedure able to check whether the above criteria are satisfied. Using the state of the art hardware and software developed in the power electronics laboratory at the Naval Postgraduate School, realistic conclusions about the performance of the electromagnetic torque estimator can be drawn. A description of the laboratory experiment tools is demonstrated below.

1. Four Pole Squirrel Cage Induction Motor

An example of a four pole squirrel cage induction motor is shown below in Figure 19.

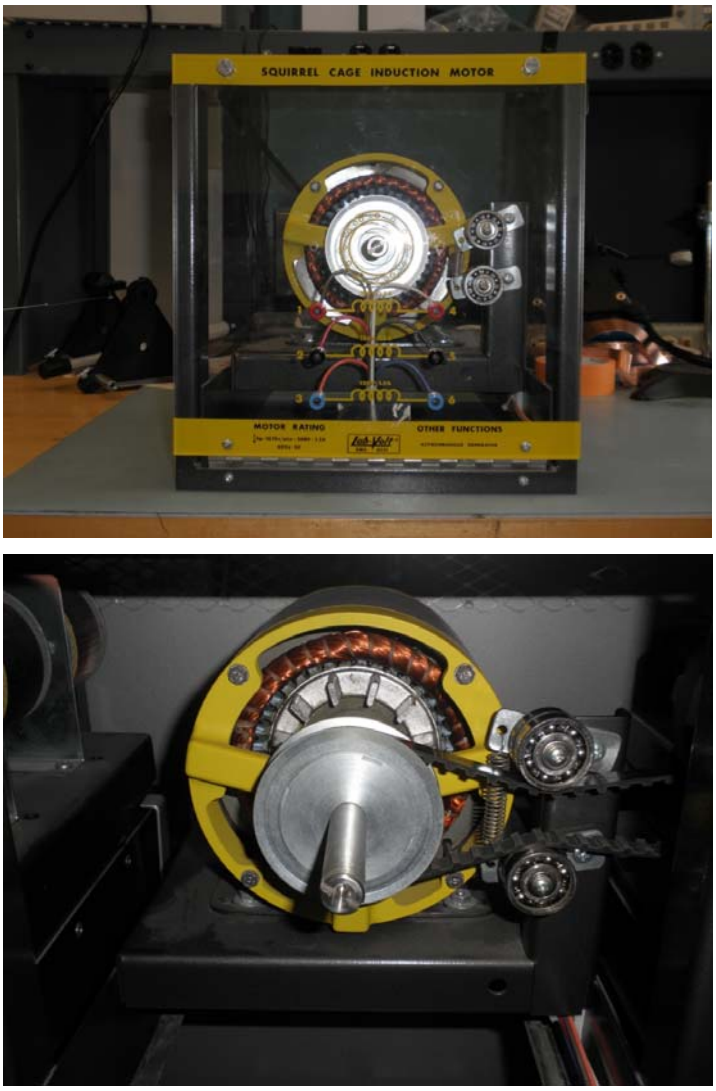

Figure 19. Model 8821 Four Pole Squirrel Cage Induction Motor

The characteristics of the experimental induction motor are displayed in Table 2.

Output Power	Stator Voltage	Frequency	Full load speed	Full load current	Dimensions	Net weight
175 W	120/208 V	60 Hz	1670r/min	1.2 A	308 x 291 x440 mm	13.5 Kg

Table 2. Characteristics of the Laboratory Induction Motor (Rating Values)

2. Electrodynamometer

In Figure 20, the electrodynamometer is connected to the motor via a belt. It applies mechanical torque to the motor that ideally is equal to the electromagnetic torque. Comparing the output of the estimator with the applied torque by the dynamometer is a way to verify its accuracy.

Figure 20. Electrodynamometer Connected to the Motor Via a Belt

3 Field Programmable Gate Array (FPGA)

The XILINX Virtex-4TM development board shown in Figure 21 incorporates the (XS4VLX25-10SF363) Field Programmable Gate Array (FPGA) as well as all the essential microelectronics in order to cooperate with multi-input logic blocks, flip-flops, multiplexors, memory and, finally, the clock generation section.

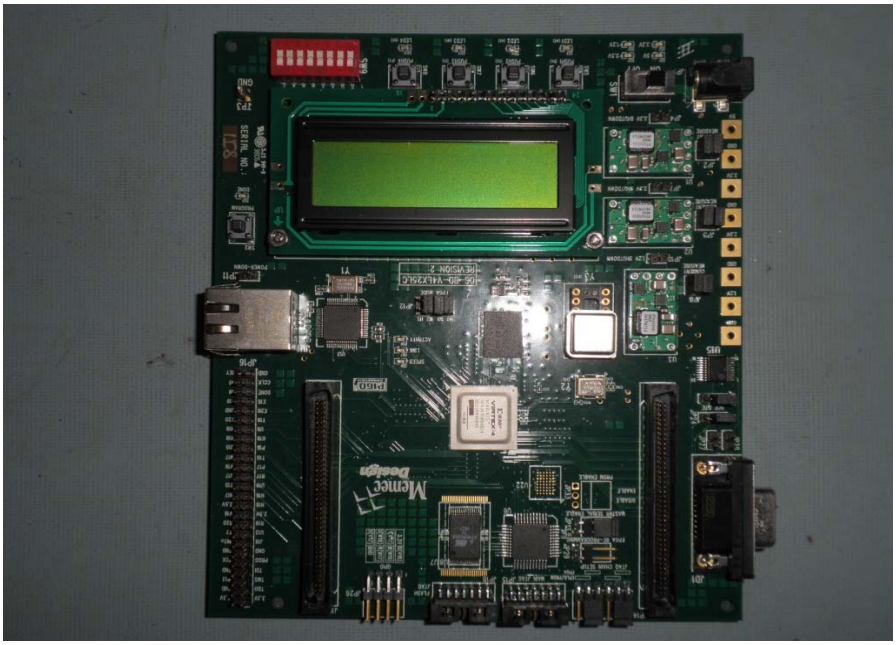

Figure 21. XILINX Virtex-4^{TM} development board

The Field Programmable Gate Array (FPGA) is the fundamental electronic tool used in our experiment. It is a semiconductor device containing programmable logic components and programmable interconnects. The distinguishing features of a FPGA are its property of being programmable by the designer and its ability to be easily reprogrammed. Using the appropriate software, this electronic device can be programmed to execute complex mathematical functions as well as combinations of them. The designed electromagnetic torque estimator is a combination of mathematical operations. Therefore, it can be implemented via the FPGA. Furthermore, the FPGA is able to execute codes in a parallel and consequently very fast manner. It can thus be connected in parallel with the motor as it runs and operates simultaneously.

4. System Interface Box

The system interface box or the FPGA development kit box in Figure 22 contains the following electronic tools:

- A power supply source that converts the input power from AC (alternate current) to DC (direct current) that is important for the safe and exact operation of the boards.
- The analogue signal interface board, which consists of eight input channels: four for the voltage and four for the current. Its main goal is to reduce the values of the input analogue signals by the appropriate ratio before their conversion from analogue to digital.
- The FPGA interface board, which contains two analogues to digital converters that sample the input signals for digital signal processing operations. Many channels are also included which can be used as outputs on the FPGA.
- The JTAG cable is used to program and reprogram the FPGA. In more general terms, the communication between the field gate array and the computer occurs through this specific cable.

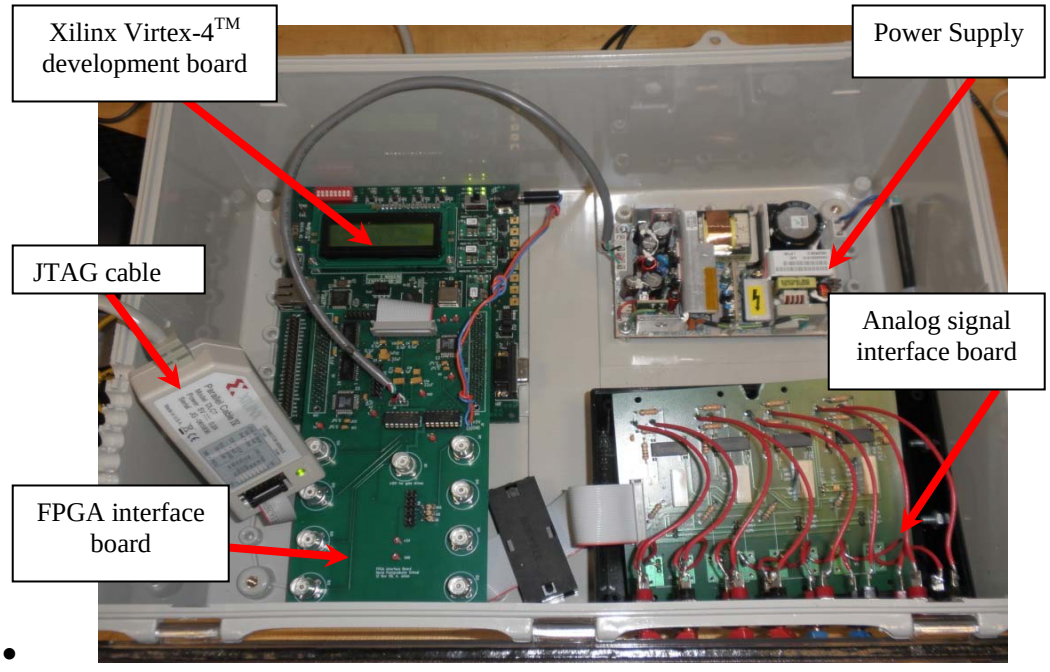

Figure 22. System Interface Box

5. Final Experiment Setup

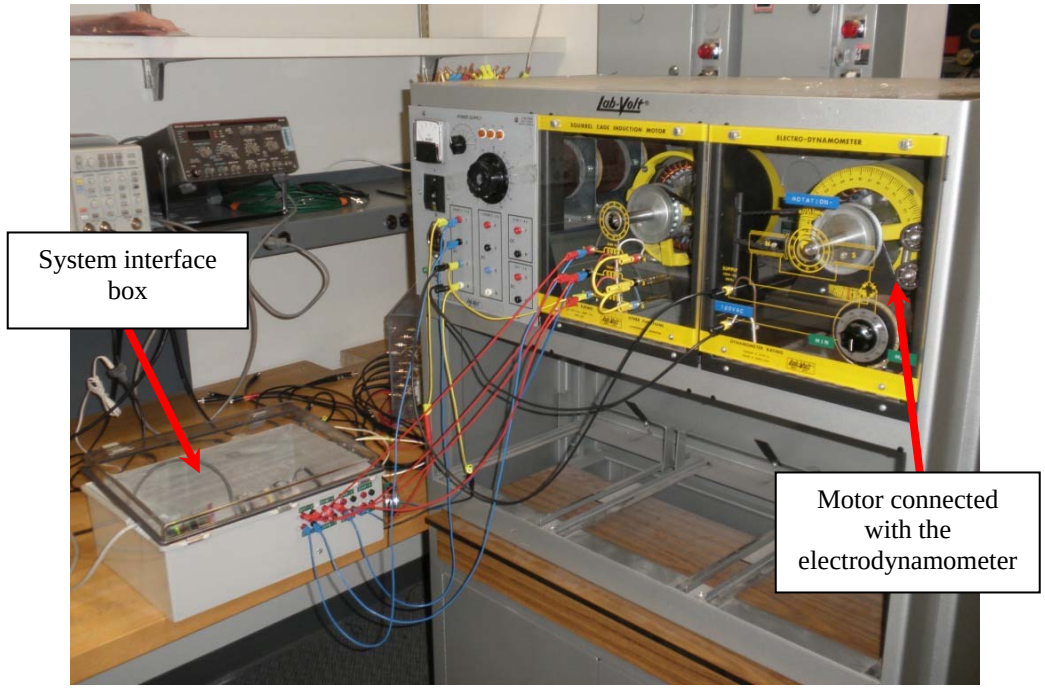

Figure 23. The Experiment Setup Station

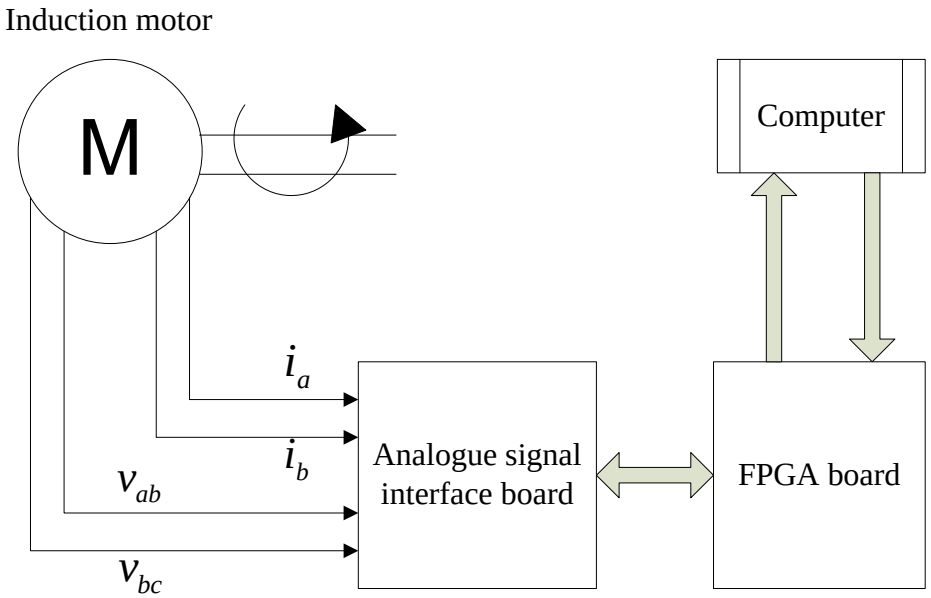

Figure 24. Schematic Diagram of the Experiment Arrangement

The experiment station is shown in Figure23 and the concept of the experiment arrangement is illustrated in the schematic diagram in Figure 24. Four channels of the analogue signal interface board are used, two for the first and second phase currents (i_a and i_b), and two for the line-to-line voltages (v_{ab} and v_{bc}). After their conversion to digital quantities, these four signals enter the FPGA. The Field Programmable Gate Array has been programmed, by using the appropriate computer software, to execute the transformation of the signals into the stationary reference frame as well as the electromagnetic torque calculation. Consequently, as the induction motor accelerates or decelerates, the FPGA calculates the electromagnetic torque continuously.

XILINX, a leading manufacturer of FPGAs, has developed the appropriate software needed for the programming of them. The proper software and the steps that are required for the final programming of the transistor are depicted in the Figure 25.

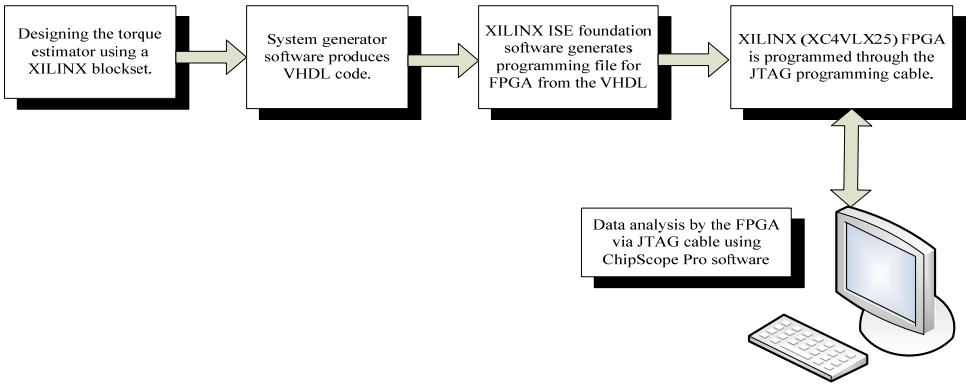

Figure 25. Programming the FPGA Using Computer Based Software

The electromagnetic torque estimator model needs to be converted in XILINX blocks using the XILINX library contained in the Simulink/Matlab library browser. Once the model has converted, the System Generator software produces the VHDL code (Very High Speed Integrated Circuit Hardware Description Language). After the VHDL is generated suitable for the FPGA files are composed by the ISE foundation software.

Through the JTAG cable the final project is uploaded in the FPGA. The results are displayed on the computer screen through the ChipScope Pro analyzer software where they can be analyzed and plotted [7].

B. XILINX SOFTWARE ANALYSIS

The Simulink/Matlab model in Figure 8 needs to be designed in XILINX environment. The designing of the XILINX library is structured in a similar way to the Simulink/Matlab library, though there are some differences in the block parameters. In fact, the XILINX library seems to be less extended compared to the Simulink/Matlab library. In addition, its capability is limited.

1. Integration in XILINX Environment

The experimental application presents certain problems caused by the external noise interference and the appearance of constant offsets at the waveforms. The flux estimation is achieved by the integration of the stationary voltage and the current waveforms. However, if there is an offset at the input of the integrator, a ramp error occurs at the output of the integration. For instance, the integration of a sine wave with an offset results in [6]:

$$\int \left(\sin(\omega t) + DC\right)dt = \int \sin(\omega t)dt + \int DCdt = -\frac{1}{\omega}\cos(\omega t) + \left(DC\right)t + Initial\ Conditions \qquad (32)$$

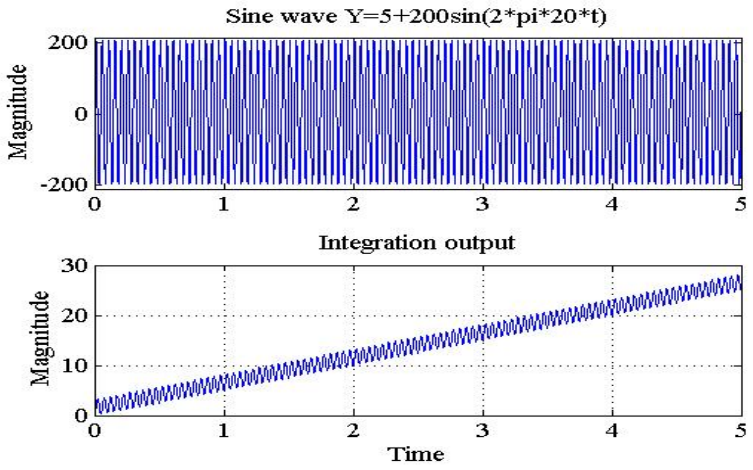

Figure 26. Ramp Error at the Output of Integration Due to an Offset in the Signal

The ramp error $(DC)t$ causes unstable integration as shown in Figure 26. This integration in turn causes saturation of the software and undesirable effects in the experimental application. Accordingly, besides the initial condition problem that arises with the low pass filter at the output, the unstable integration problem needs to be overcome.

The integration output can become stable by applying a unity feedback as shown in Figure 27.

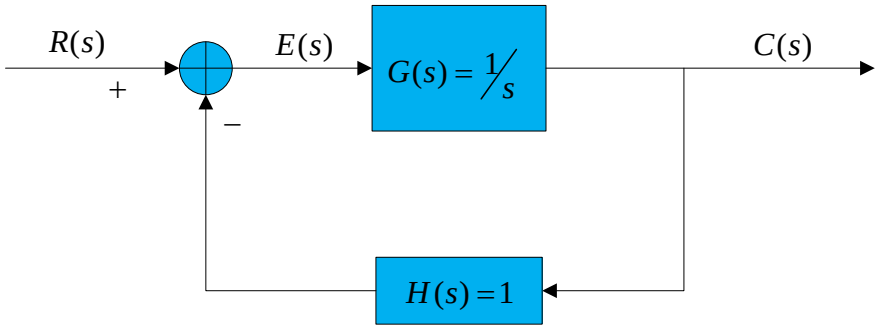

Figure 27. Closed loop system with unity feedback

The transfer function of the unity feedback closed loop system becomes:

$$Tf = \frac{C(s)}{R(s)} = \frac{G(s)}{1+G(s)H(s)} = \frac{1/s}{1+1/s} = \frac{1}{s+1} \qquad (33)$$

As derived from the analysis above, the application of the operator ($1/s+1$) instead of the operator ($1/s$) gives a stable integration output as shown in Figure 28. Thus, the flux integrator in XILINX software is going to be implemented as ($1/s+1$).

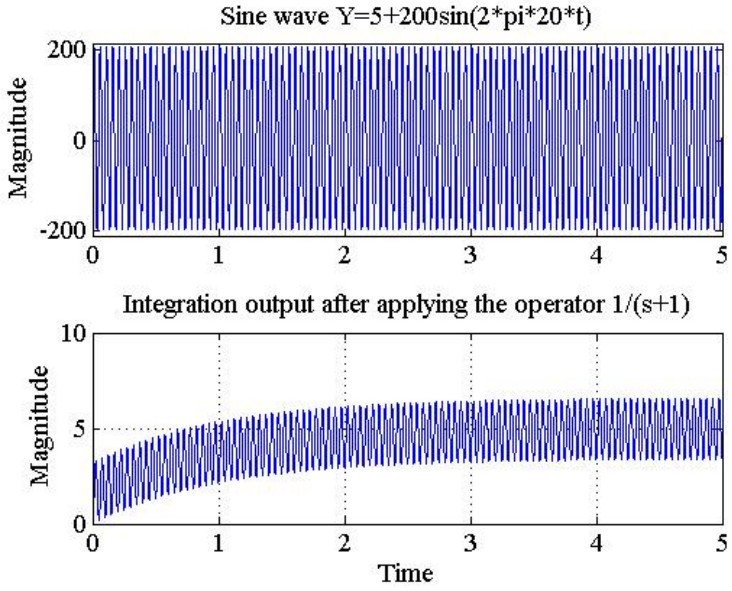

Figure 28. The Operator ($1/s+1$) Makes the Integration Stable

The implementation of the integral operator $1/s+1$ in real time application is yet another problem to be sorted out. In general, the digital implementation includes several hardware limitations, such as limited memory, finite precision, and limited speed execution. Operations that require a finite amount of data and make the algorithm computable are necessary.

According to the Euler approximation technique, a transfer function in the differential operator (s) can be transformed into a discrete time transfer function in the time delay operator (z) by substituting [4]:

$$s = \frac{1 - z^{-1}}{T_s} \qquad (34)$$

In equation (34) T_s is the sampling interval. The clock frequency of the FPGA is 25 MHz and consequently the sampling interval is 40×10^{-9} sec.

By substituting equation (34) in the integral operator $1/s+1$, it is obtained:

$$\frac{1}{s+1} = \frac{1}{\frac{1-z^{-1}}{T_s}+1} = \frac{1}{\frac{1-z^{-1}}{40\times10^{-9}}+1} = \frac{4\times10^{-8}}{1.00000004 - z^{-1}} = \frac{3.99\times10^{-8}}{1-0.99999996z^{-1}} \qquad (35)$$

In time domain equation (35) is implemented by the difference equation:

$$y[n] = 0.99999996\,y[n-1] + 3.99x10^{-8}\,x[n] \qquad (36)$$

Equation (36) yields the following block diagram realization:

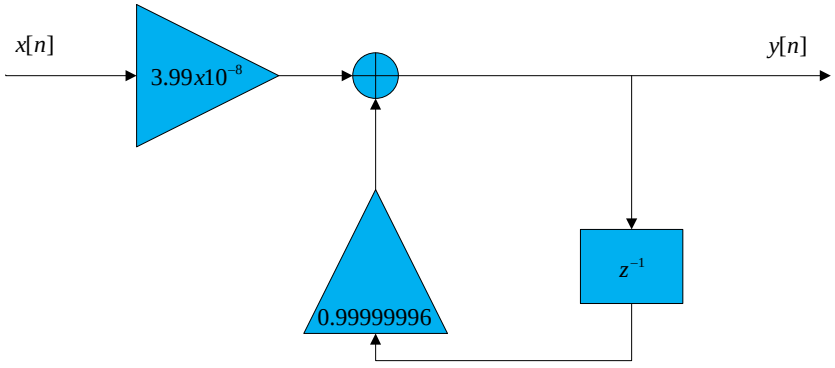

Figure 29. Block diagram realization of equation (36)

The block diagram above in Figure 29 represents the operator $1/(s+1)$ with elementary operations such as the time delay, sum and scaling, which use the minimum memory storage. It can be used in our real time application. The integrator in XILINX software has been designed based on this concept and it is shown in Figure 30.

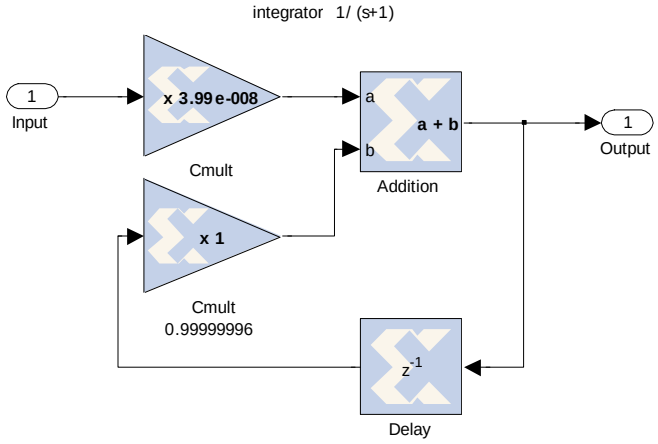

Figure 30. Integrator in XILINX Environment

2. Low Pass Filter in XILINX Environment

The construction of the low pass filter at the output of the electromagnetic torque estimator is based on the same concept. Instead of a second order filter, which complicates the design, two cascaded first order low pass filters with transfer function $Tf = \frac{10}{s+10}$ are implemented. The designed filter is shown in Figure 31.

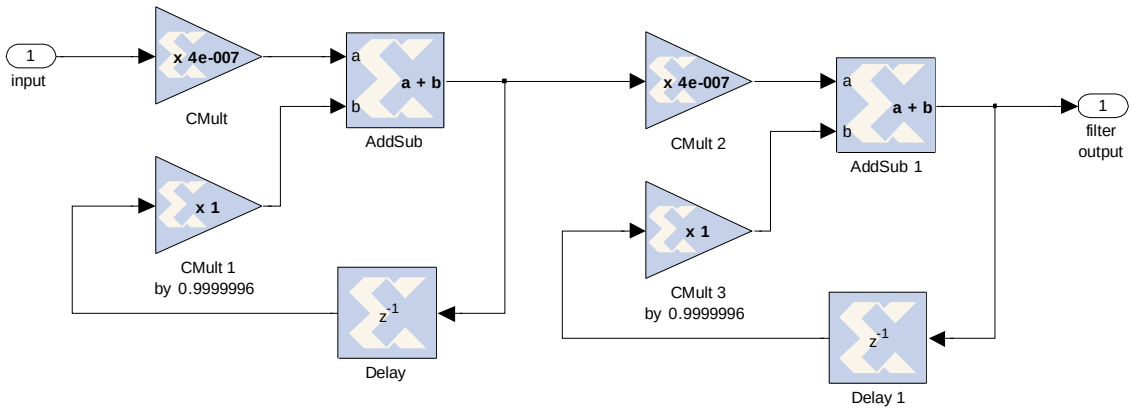

Figure 31. Two Cascaded First Order Low Pass Filters using XILINX Blocks

3. Final Design of the Torque Estimator in XILINX Environment

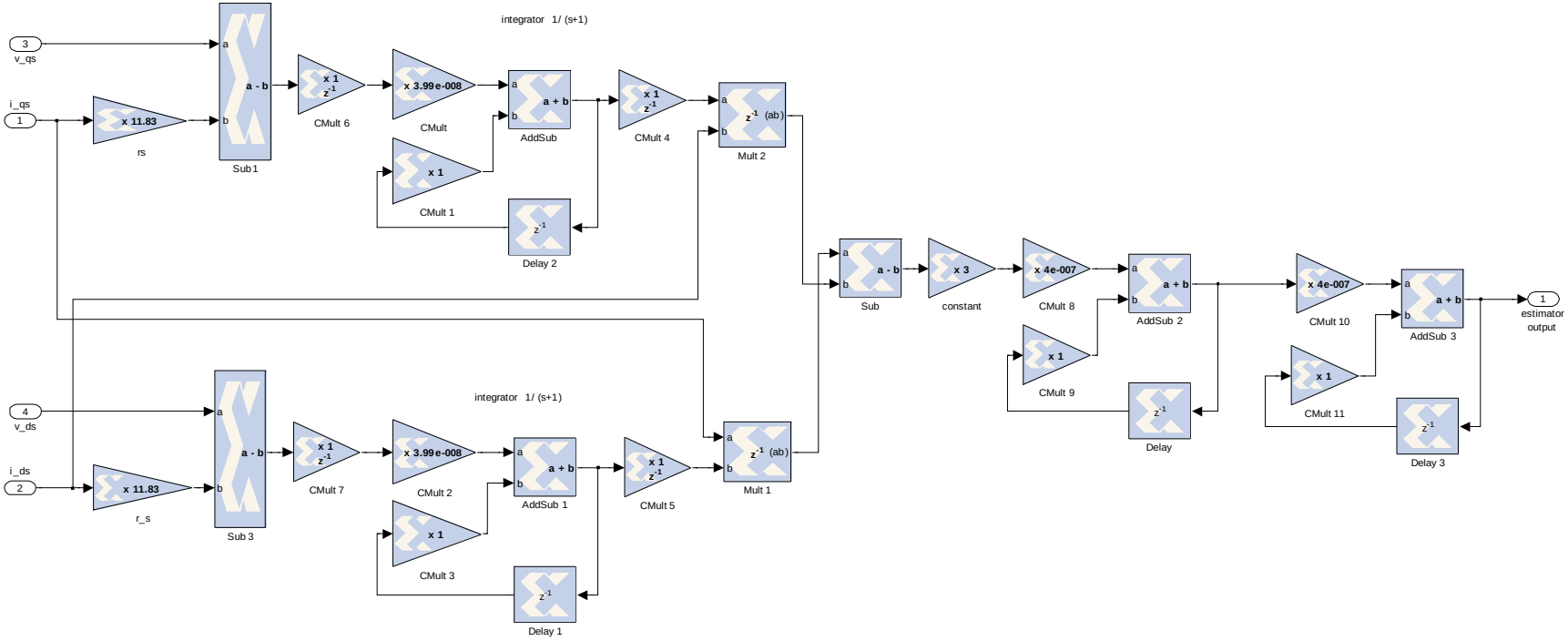

Figure 32. Electromagnetic Torque Estimator Converted in XIILINX Environment

The complete design of the electromagnetic torque estimator is illustrated in Figure 32.

4. Implementation of Transformations using XILINX Software

The first and second phase currents (i_a and i_b), as well as the line-to-line voltages (v_{ab} and v_{bc}), have been defined as the four inputs on the analogue interface board. Nevertheless, these quantities must be transformed into the stationary reference frame. This transformation is going to be achieved through the FPGA by designing the proper software using XILINX blocks.

The equations that describe the q-axis and d-axis stator currents as a function of the stator currents (i_a and i_b) are respectively [2]:

$$i_{qs} = \frac{2\sqrt{3}}{3}\sin(\theta + \frac{\pi}{3})i_a + \frac{2\sqrt{3}}{3}\sin(\theta)i_b \qquad (37)$$

$$i_{ds} = -\frac{2\sqrt{3}}{3}\cos(\theta + \frac{\pi}{3})i_a - \frac{2\sqrt{3}}{3}\cos(\theta)i_b \qquad (38)$$

Substituting ($\theta = 0$) in equations (37) and (38), the stator currents are transformed from the arbitrary into the stationary reference frame. The XILINX software, which transforms the stator currents into the stationary reference frame, is based on equations (37) and (38) is shown in Figure 33.

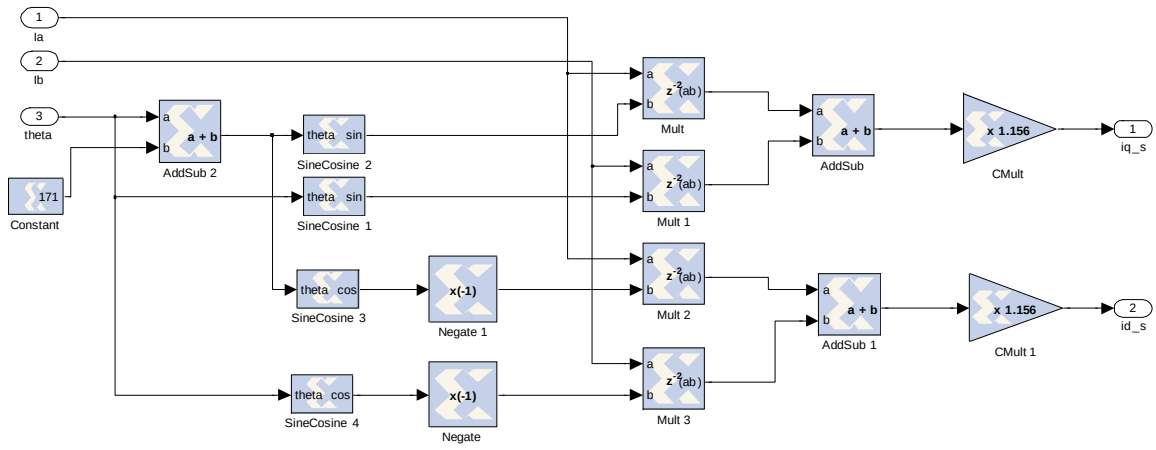

Figure 33. Software that Transforms the Stator Currents (i_a and i_b) into the Stationary Reference Frame (From [2])

The equations that describe the q-axis and d-axis stator voltages as a function of the stator line-to-line voltages are respectively [2]:

$$v_{qs} = \frac{2}{3}\cos(\theta)v_{ab} + \frac{2}{3}\sin(\theta + \frac{\pi}{6})v_{bc} \qquad (39)$$

$$v_{ds} = \frac{2}{3}\sin(\theta)v_{ab} - \frac{2}{3}\cos(\theta + \frac{\pi}{6})v_{bc} \qquad (40)$$

Consequently, the final model, which transforms the line-to-line stator voltages into the stationary reference frame, is based on the equations (39) and (40) as seen in Figure 34.

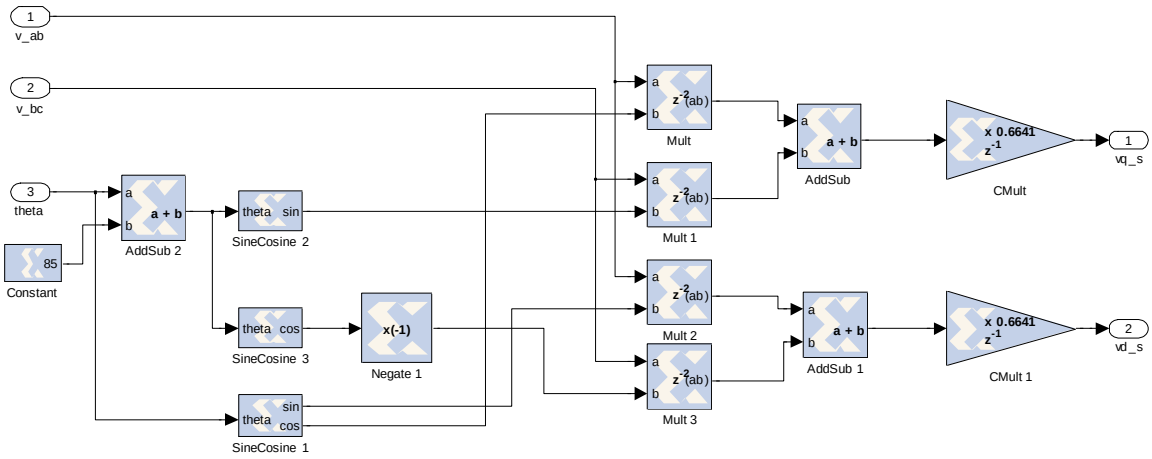

Figure 34. Software that Transforms the Line-to-Line Voltages (v_{ab} and v_{bc}) into the Stationary Reference Frame (From [2])

IV. EXPERIMENTAL RESULTS AND ANALYSIS

The analysis of the experimental results can be done on the computer using ChipScope Pro software. ChipScope Pro inserts a logic analyzer and a bus analyzer core directly into the design. This allows the user to view any internal signal through the programming interface and analyze it with the ChipScope Pro Logic Analyzer. Furthermore, the data can be exported to Matlab environment for measuring and plotting [7].

The accuracy of the electromagnetic torque estimator is going to be verified by the electrodynamometer. The electrodynamometer is connected to the motor via a belt. It applies mechanical torque to the motor that, ideally, is equal to the electromagnetic torque. In practice, the measured electromagnetic torque should be a little bit larger in order to get over the mechanical load and the losses. However, the difference is insignificant. Thus, the electrodynamometer is a good way to test the electromagnetic torque estimator. On the electrodynamometer, there is an indicator that shows the applied mechanical torque in pound force inches ($lbf.in$). In addition, a rotational knob allows the user to apply step loads to the motor.

The applied stator phase voltage is $V_{phase,RMS} = 110 Volt$. The rating value is $V_{phase,RMS} = 120 Volt$. As the motor is connected to the electrodynamometer, even if there is no load applied, it has an initial electromagnetic torque in order to turn itself as well as the electrodynamometer. This torque needs to be measured. Furthermore, it is necessary for this value to be added to the applied mechanical load and this addition in turn should be compared with the estimator measurement.

The measured initial electromagnetic torque is $2.4\,lbf.in$, as seen in Figure35.

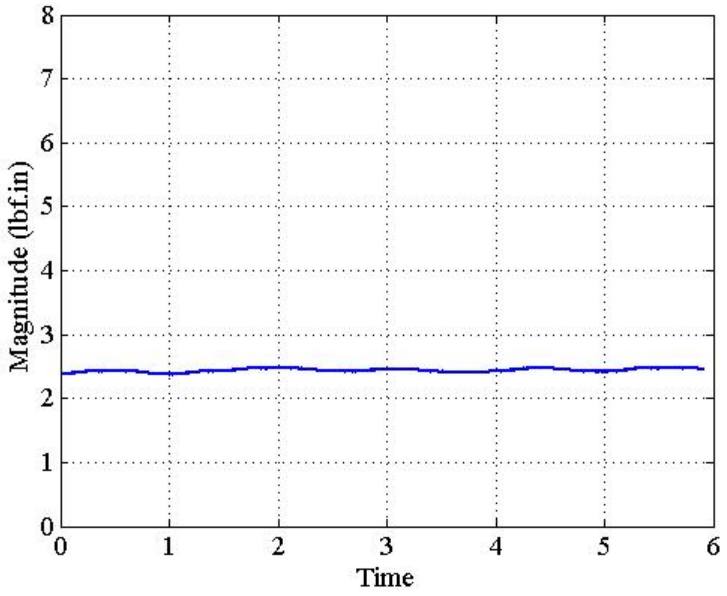

Figure 35. Measured electromagnetic torque of the motor in zero load condition

The rating stator current is $I_{stator} = 1.2\,Amperes$. According to this limitation, the maximum mechanical torque that can be applied is $10\,lbf.in$. So three step loads below $10\,lbf.in$ are applied to the motor in order to test the electromagnetic torque estimator.

The electromagnetic torque waveform after applying a $3\,lbf.in$ step load for the time interval of four seconds and back again to zero load is displayed in Figure 36. Following the same procedure, the torque waveforms after applying $6\,lbf.in$ and $10\,lbf.in$ step loads are shown in Figure 38 and Figure 40 respectively.

The measured steady state electromagnetic torque at $3\,lbf.in$, $6\,lbf.in$ and $10\,lbf.in$ loads is displayed in Figure 37, Figure 39 and Figure 41 respectively. The measured values approximate the corresponding actual values and that verifies the accuracy of the designed electromagnetic torque estimator.

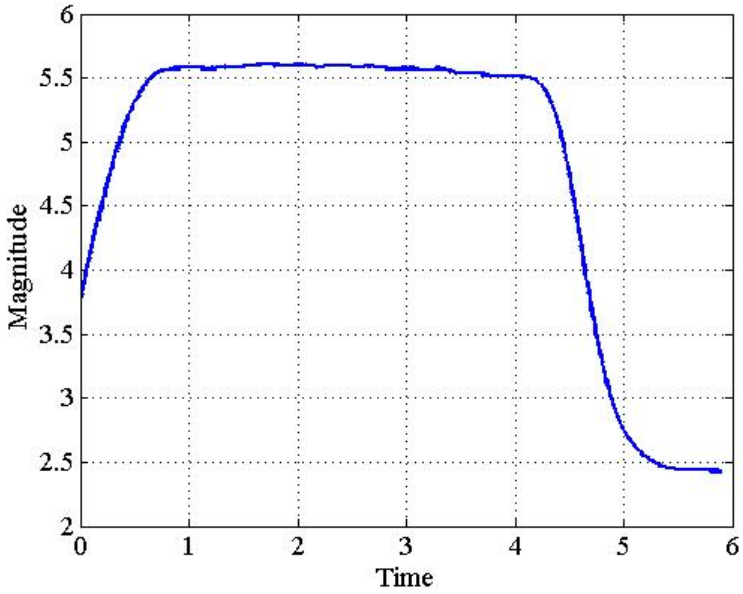

Figure 36. Electromagnetic Torque Waveform after Applying $3\,lbf.in$ Load and Back again to Zero Load

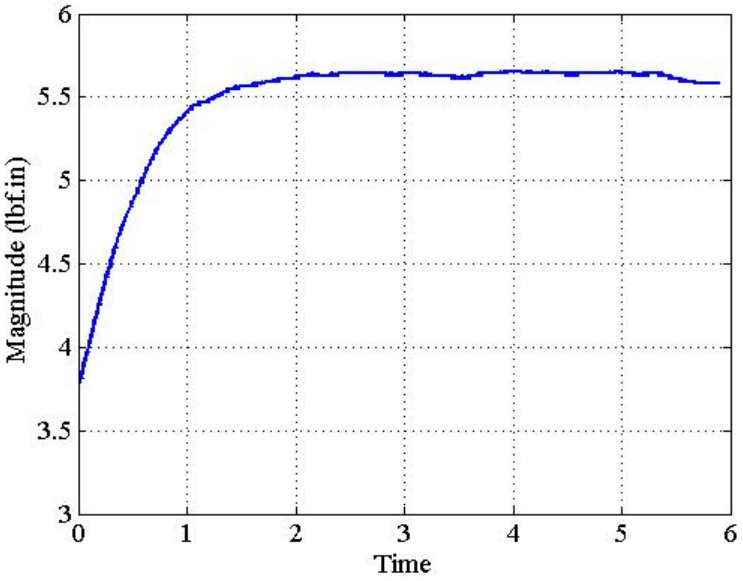

Figure 37. Transient and Steady State Response of the Electromagnetic Torque after Applying a Step Load of $3\,lbf.in$

As derived from Figure 37 the measured steady state torque is $5.6\,lbf.in$, approximate to the actual value of $5.4\,lbf.in$.

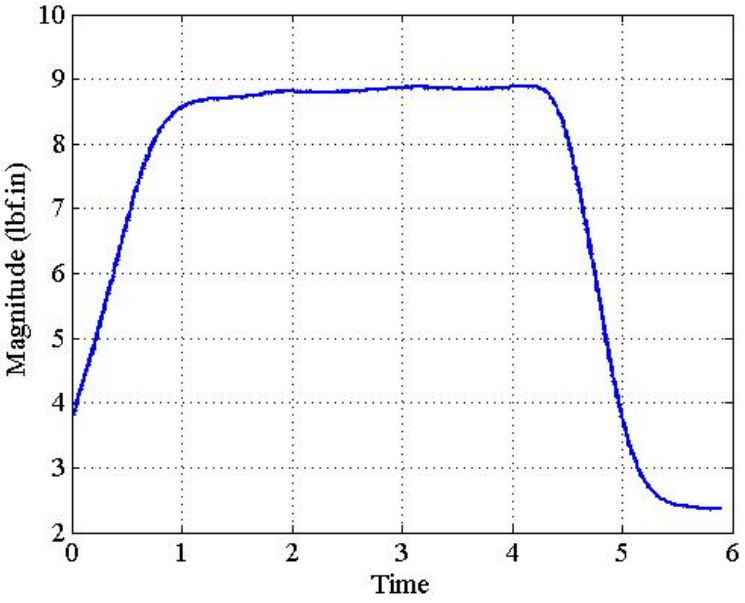

Figure 38. Electromagnetic Torque Waveform after Applying 6 *lbf .in* Load and Back again to Zero Load

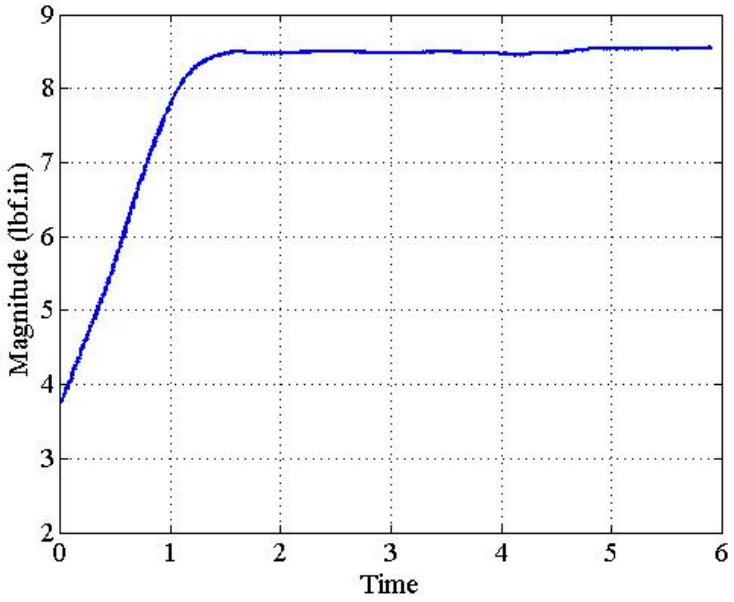

Figure 39. Transient and Steady State Response of the Electromagnetic Torque after Applying a Step Load of 6 *lbf .in*

The measured steady state torque as shown in Figure 39 is 8.5 *lbf .in* as expected.

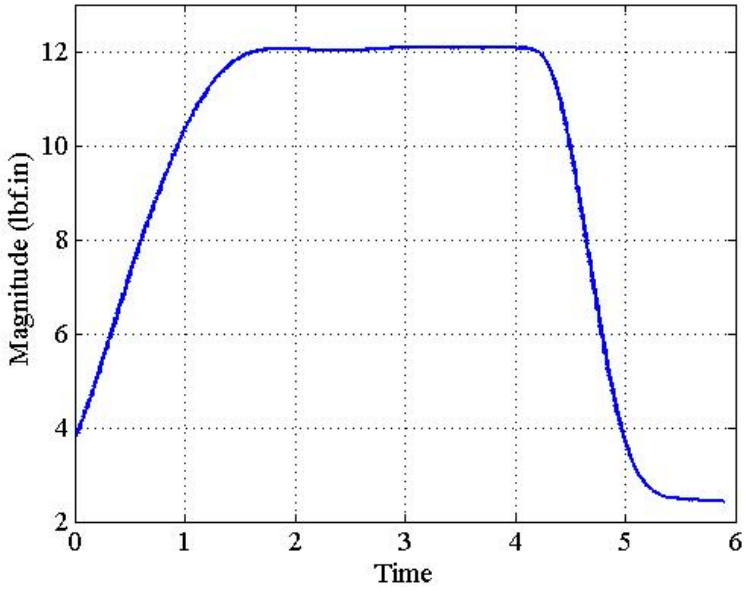

Figure 40. Electromagnetic Torque Waveform after Applying 10 *lbf .in* Load and Back again to Zero Load

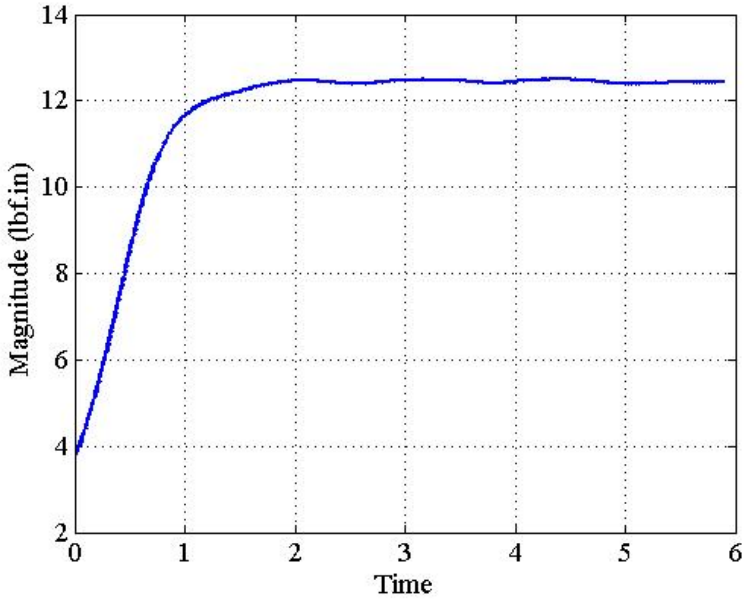

Figure 41. Transient and Steady State Response of the Electromagnetic Torque after Applying a Step Load of 10 *lbf .in*

As derived from Figure 41 the measured steady state torque is 12.5 *lbf .in* , approximate to the actual value of 12.4 *lbf .in* .

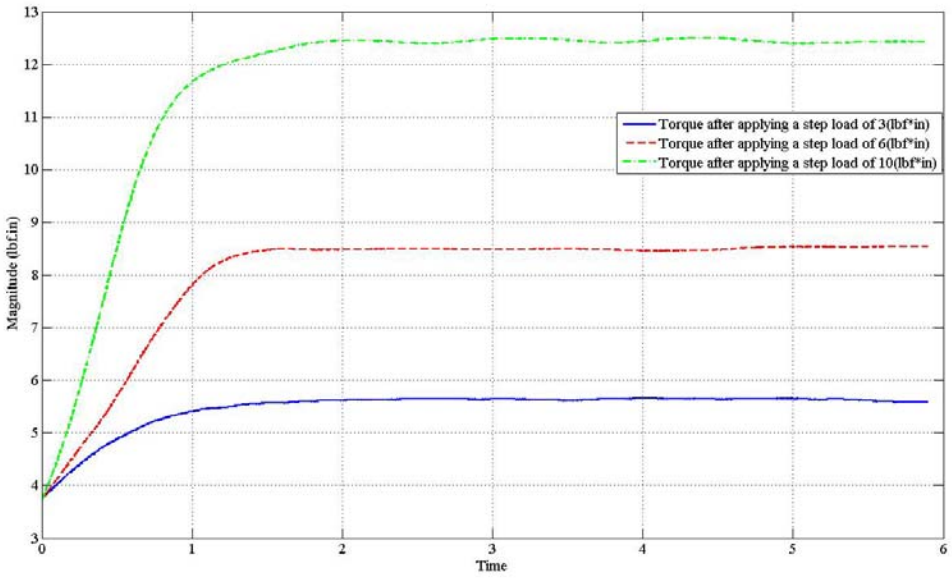

Figure 42. Response of the Electromagnetic Torque to Three Different Loads

The steady state values of the three different step loads are shown in Figure 42. The calculated steady state torque approximates the electrodynamometer settings. The analysis of the results shows that the torque estimator works successfully for the induction motor.

A comparison of the measured electromagnetic torque waveforms with the computer simulation results cannot be accomplished, due to the unknown machine parameters and inertia of the laboratory induction motor.

V. CONCLUSIONS AND SUGGESTIONS

A. CONCLUSIONS

The quality and reliability of any design are proven by how well it works in a real application. The transition from an ideal case, such as computer simulation, to a real application includes factors that may have undesirable effects. The experiment of an electromagnetic torque estimator using a real induction motor is a real application which involves undesirable external noise, constant offsets at the waveforms, as well as variation in the temperature of the windings and thus in the stator resistance. Nevertheless, the analysis of the results shows that the torque estimator works very well for an induction motor at the frequency of 60 Hz. The calculated steady state torque is very close to the electrodynamometer settings. In conclusion, at the speed of 60 Hz the variation of the stator resistance is not dominant and does not affect the torque calculation. Finally, the numerical integration works successfully.

The designed torque estimator can be used in any application that requires the calculation of the torque of an induction motor that works at a high frequency. In fact, the calculation of the electromagnetic torque is an important step before the speed control of the motor. The speed of the motor can be controlled by controlling how much electromagnetic torque is applied on the induction motor. Such a direct torque control scheme works very successfully only if the estimation of the torque is accurate.

B. SUGGESTIONS FOR FURTHER RESEARCH

At low frequencies, the estimation of the flux becomes difficult. Two important negative effects render the designed torque estimator less efficient: the low pass filter, which should have low cutoff frequency, as well as the small transition region, which causes complexity problems. Therefore, instead of a low pass filter, a detector could be designed to detect the initial conditions of the flux and remove them before integration.

An equally important problem caused by the low frequency is the stator resistance variation. The voltage drop across the stator resistance is comparable to the applied voltage due to the high stator current. Therefore, any variation in the stator resistance would cause an error in the flux estimation. In this case, an algorithm that could compute the variations of the resistance would improve the performance of the electromagnetic torque estimator.

APPENDIX: COMPUTER SIMULATION MODEL

Induction machine model

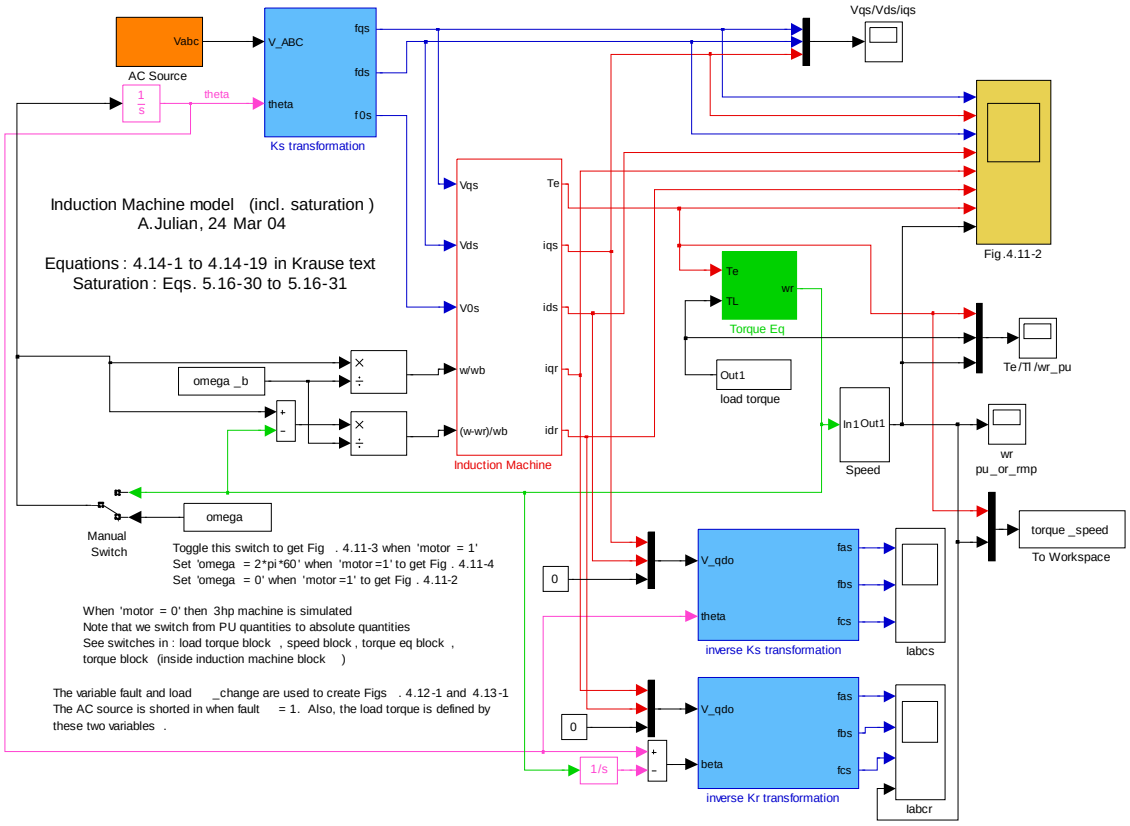

Induction machine model/AC source

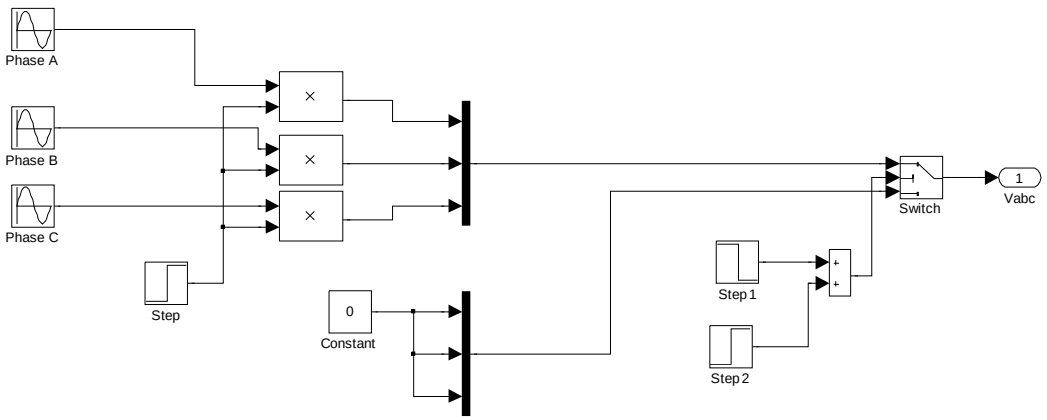

Induction machine model/Induction Machine

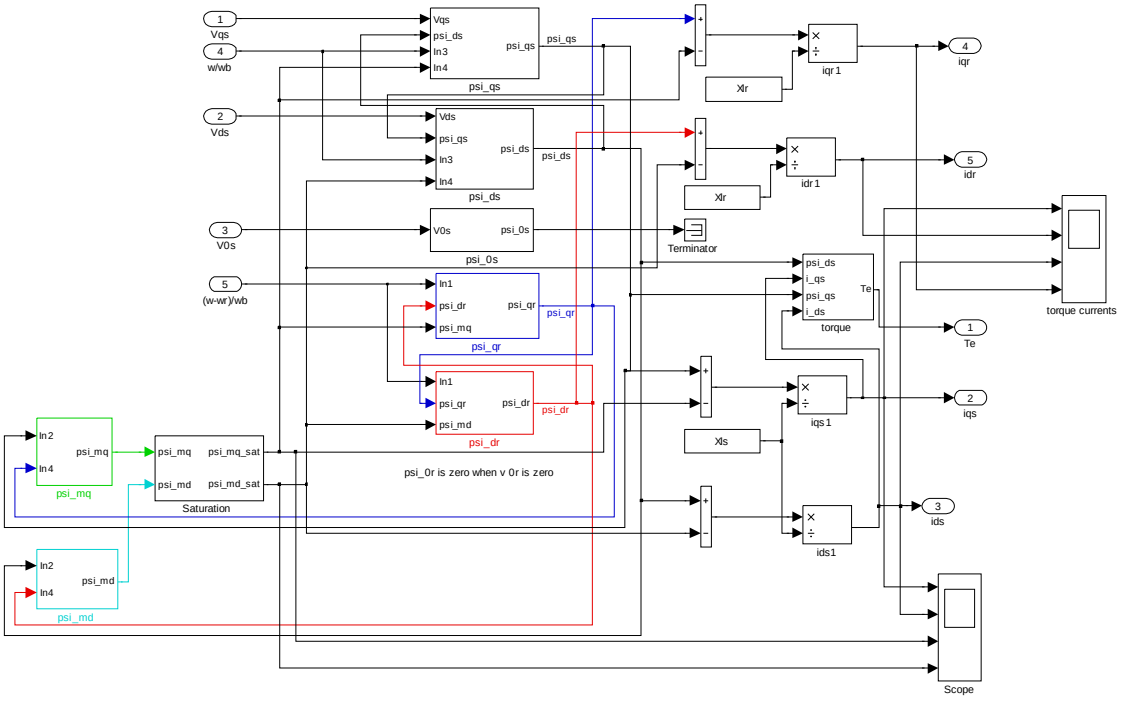

Induction machine model/Induction machine/Saturation

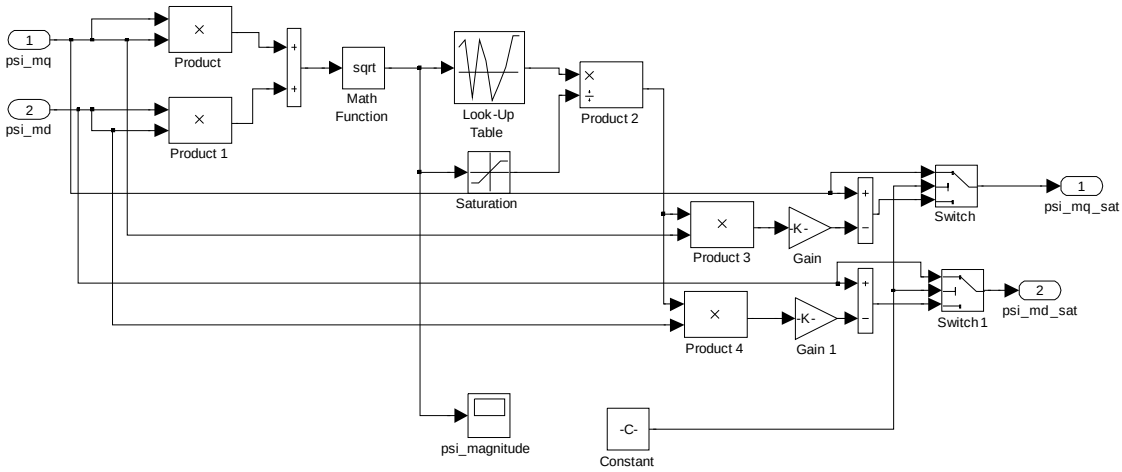

Induction machine model/Induction machine/psi_0s

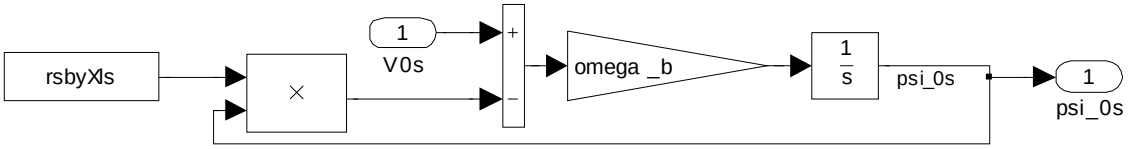

Induction machine model/Induction machine/psi_dr

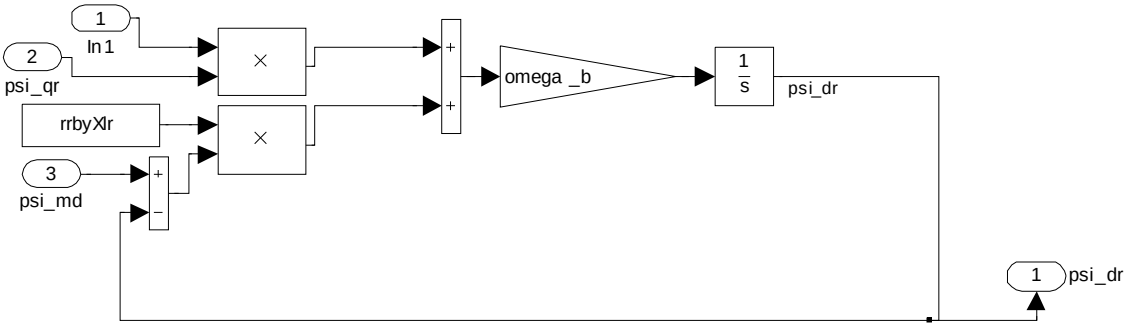

Induction machine model/Induction machine/psi_ds

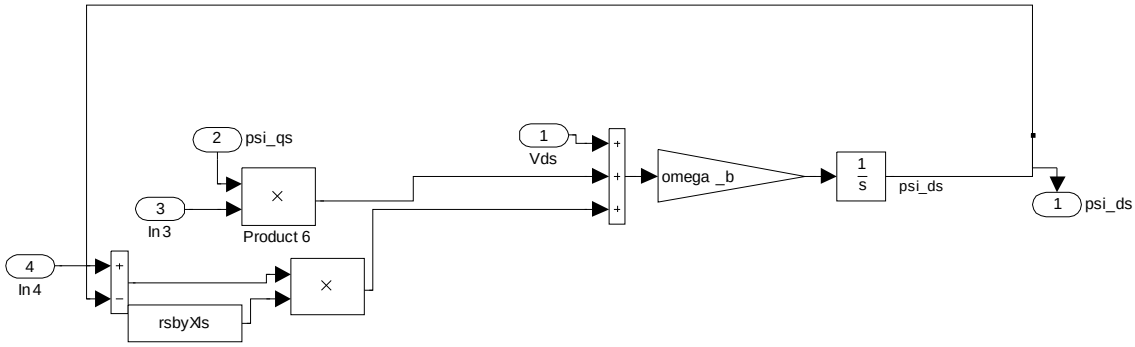

Induction machine model/Induction machine/psi_md

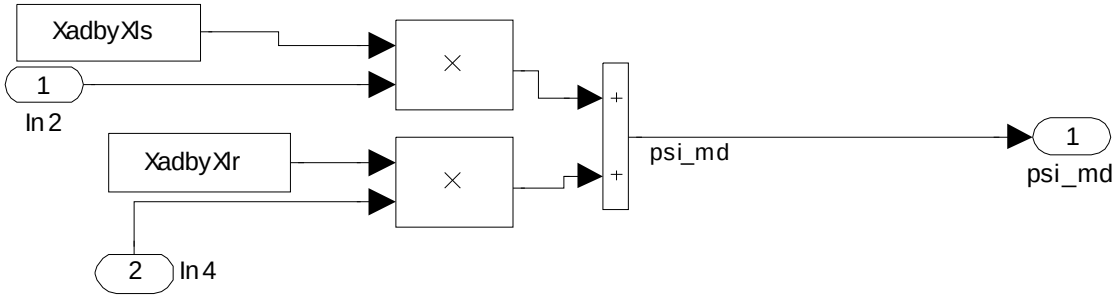

Induction machine model/Induction machine/psi_mq

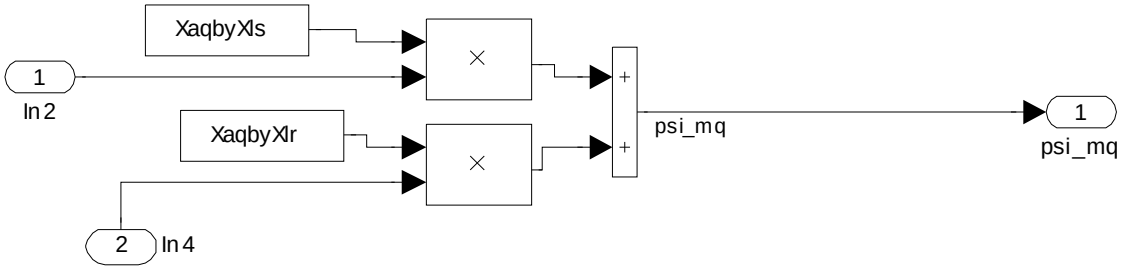

Induction machine model/Induction machine/psi_qr

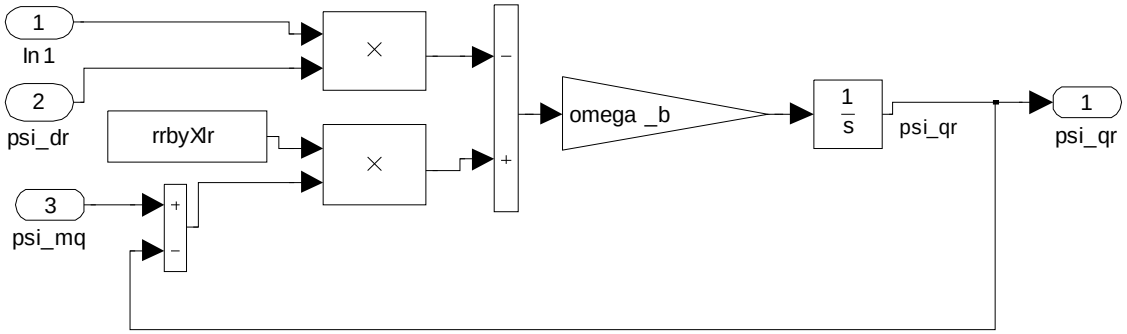

Induction machine model/Induction machine/psi_qs

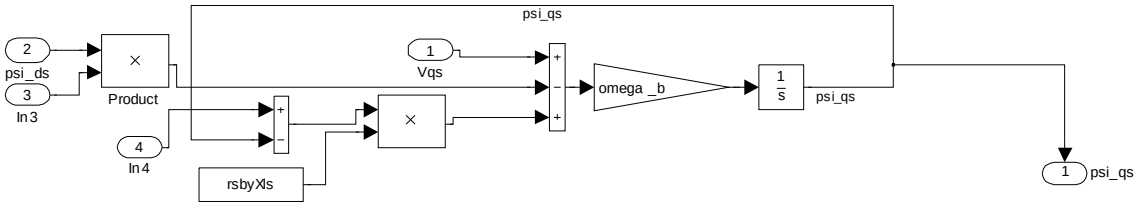

Induction machine model/Induction machine/torque

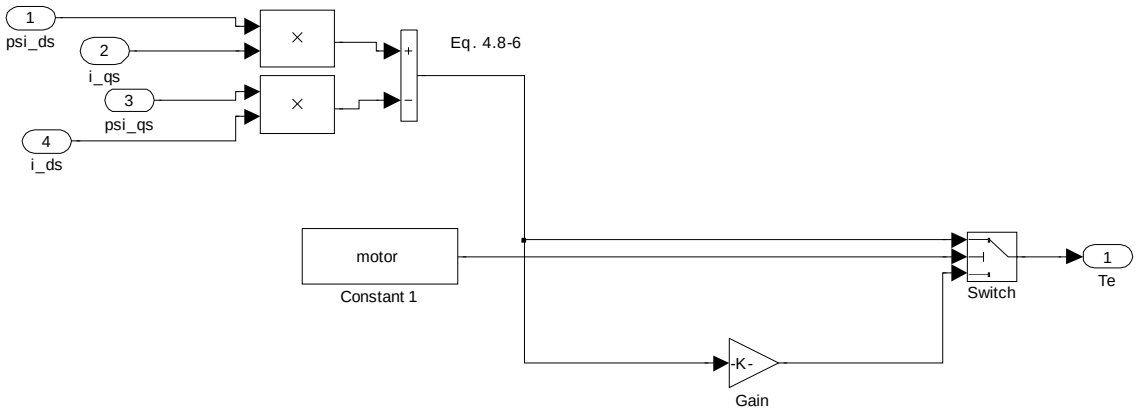

Changes electrical torque from perunit to absolute values
Eq. 4.6-5

Induction machine model/Ks transformation

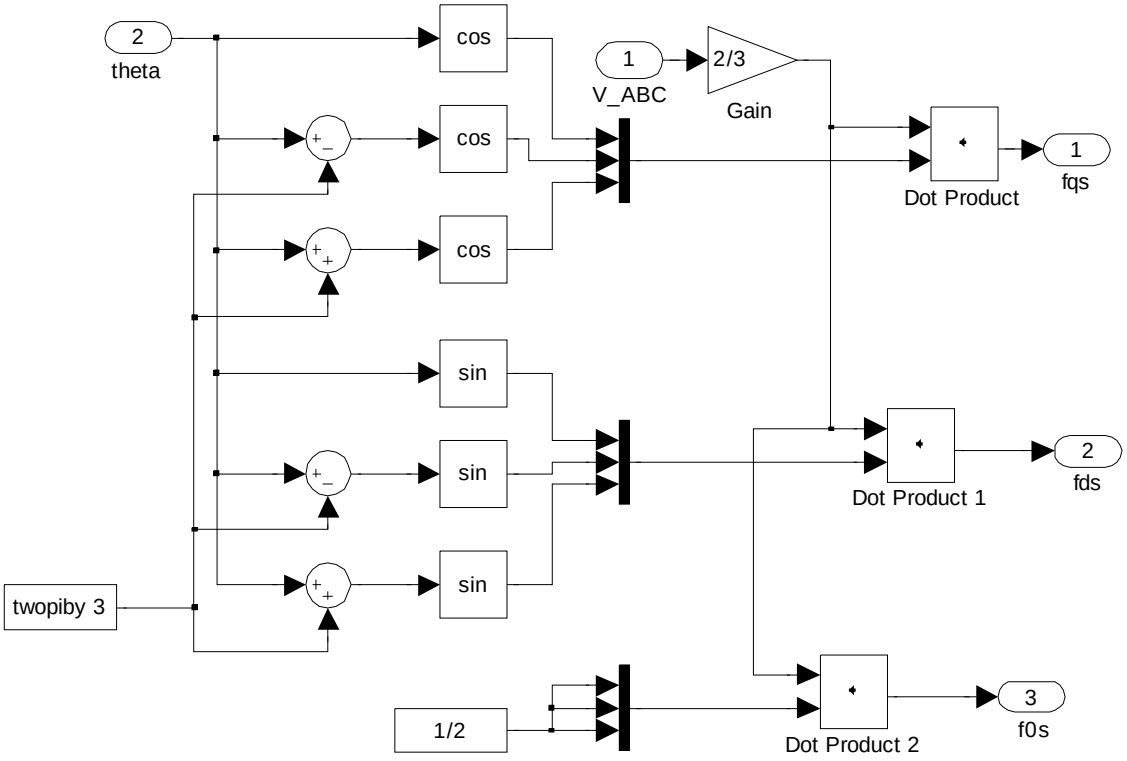

Induction machine model/speed

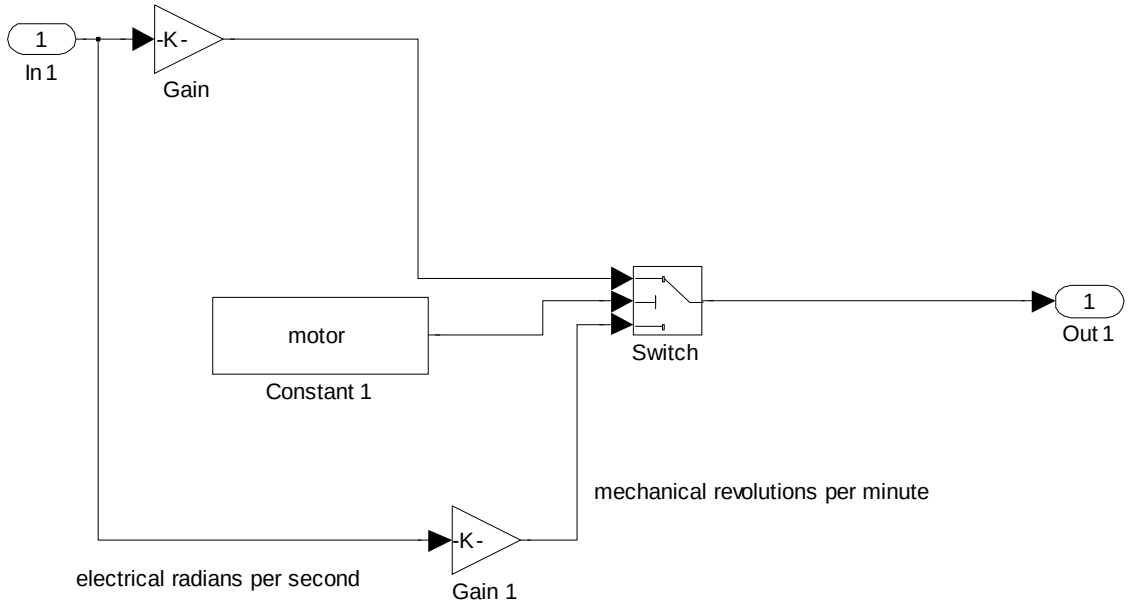

Induction machine model/Torque Eq

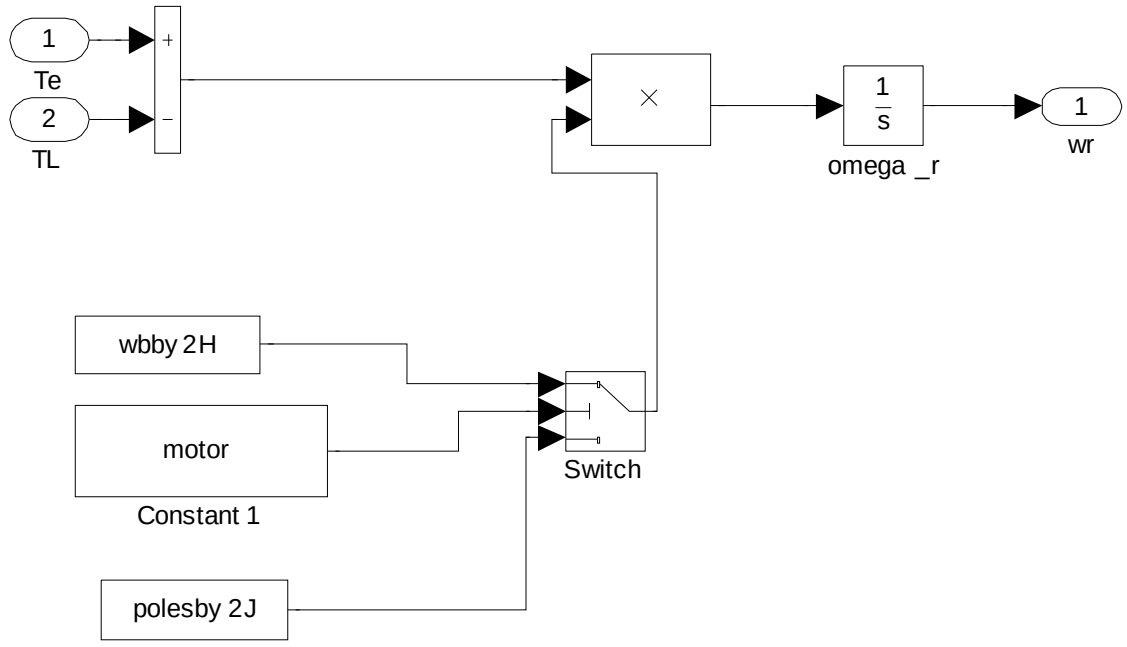

Induction machine model/inverse Kr transformation

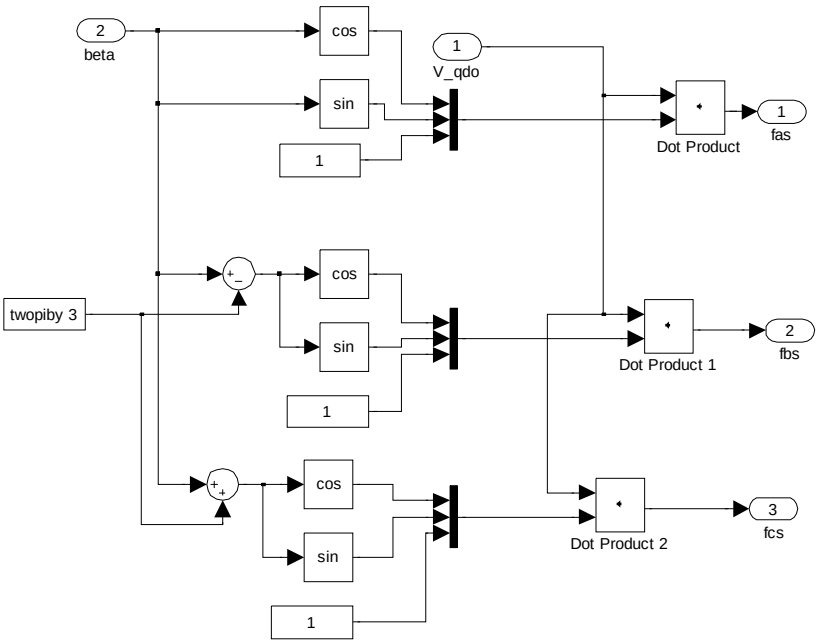

Induction machine model/inverse Ks transformation

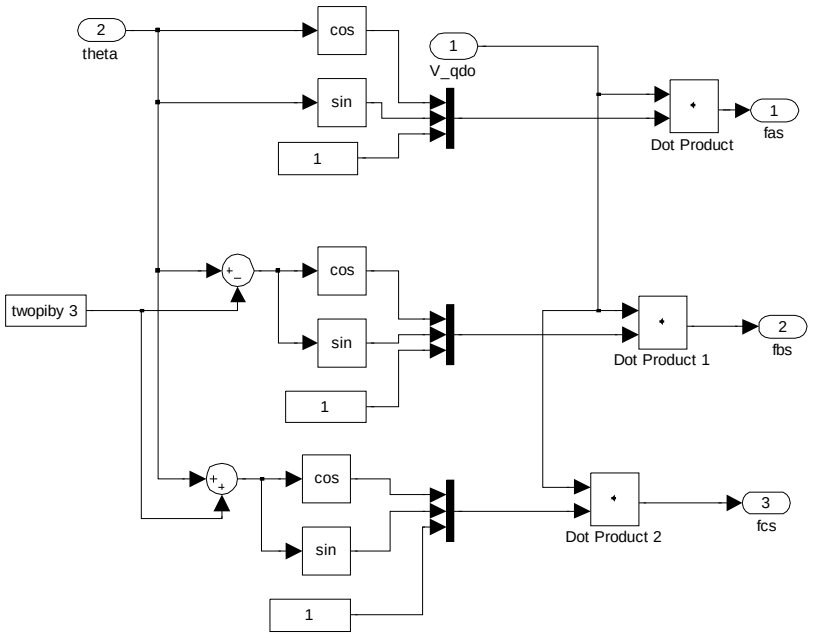

Induction machine model/load torque

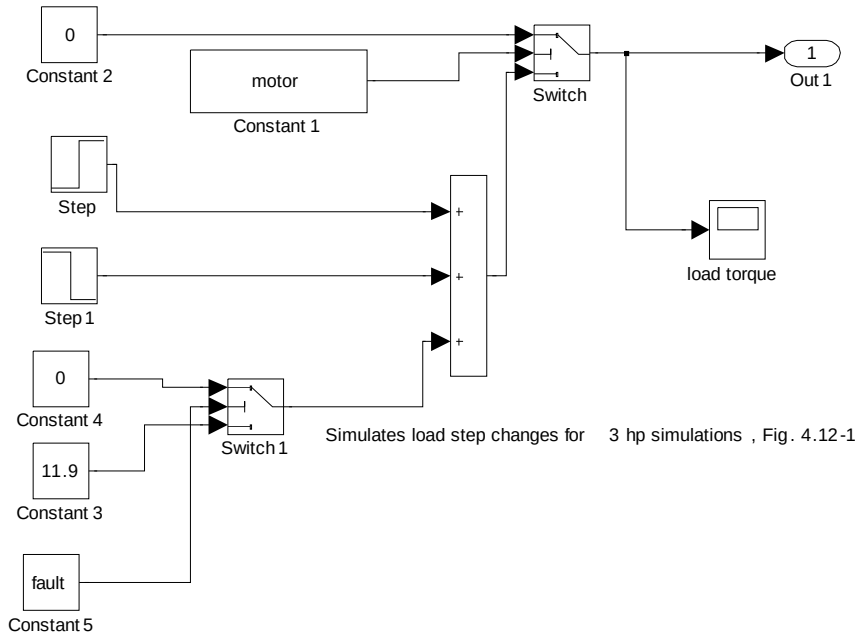

Initial Matlab file

```
motor = 0;  %when motor = 1 then 10 HP machine, motor = 0 then 3 hp
machine
saturation = 1; %OFF when set to one, ON when set to zero
tfault_on = 30.75/60;   %page 181 to describe fog. 4.13-1
tfault_off = 36.75/60;
%omega = 2*pi*60;  %Modify this variable to change reference frame
omega = 0;  %Modify this variable to change reference frame
omega_b = 2*pi*60;
omega_in = 2*pi*60;
t_start = .1;
tstep=.000002;
twopiby3 = 2*pi/3;
wbby2H = omega_b/2/0.5;
poles = 4;
polesby2J = poles/2/.089;
fault_or_loadchange =0; %Fault when 1, load change when not=1
if fault_or_loadchange == 1
    fault = 1;    % set to large value to disable (like 100)
    load_change = 100;
else
    fault = 100;    % set to large value to disable (like 100)
    load_change = 1;
end
if motor ==1
%Parameters from section 4.11, 10 HP machine
tfault_on = 100*30.75/60;   %page 181 to describe fig. 4.13-1
tfault_off = 100*36.75/60;
tstep=.00002;
tstop=.9;
rs=.0453;
rr = .0222;
Xls =.0775;
Xm =2.042;
Xlr = .0322;
rsbyXls = rs/Xls;
rrbyXlr = rr/Xlr;
Xaq = 1/(1/Xm+1/Xls+1/Xlr);
Xad = Xaq;
XaqbyXls = Xaq/Xls;
XaqbyXlr = Xaq/Xlr;
XadbyXls = Xad/Xls;
XadbyXlr = Xad/Xlr;
XaqbyXm = Xaq/Xm;
XadbyXm = Xad/Xm;
V_phase = 1;
psi_mqic=0;
psi_mdic=0;
psi_qsic=0;
psi_dsic=0;
psi_qric=0;
```

```
psi_dric=0;
omegar_ic = 0;
elseif motor == 0
%Parameters from section 4.10, 3 HP machine
t_start = 0;
tstop=1.6;
rs=.435;
rr = .816;
Xls =.754;
Xm =26.13;
Xlr = .754;
rsbyXls = rs/Xls;
rrbyXlr = rr/Xlr;
Xaq = 1/(1/Xm+1/Xls+1/Xlr);
Xad = Xaq;
XaqbyXls = Xaq/Xls;
XaqbyXlr = Xaq/Xlr;
XadbyXls = Xad/Xls;
XadbyXlr = Xad/Xlr;
XaqbyXm = Xaq/Xm;
XadbyXm = Xad/Xm;
V_phase = 220*sqrt(2)/sqrt(3);  %Peak value used in Simulink for source
model

%Steady state analysis
omega_rotor = .999*omega_in;
slip = (omega_in-omega_rotor)/omega_in;
Z1 = rs + j*omega_in/omega_b*Xls;
Z2 = j*omega_in/omega_b*Xm;
Z3 = rr/slip + j*omega_in/omega_b*Xlr;
Ias = V_phase/sqrt(2)/(Z1 + Z2*Z3/(Z2+Z3));
Iar = -Ias*(Z2*Z3/(Z2+Z3))/Z3;
Te = 3*poles/2*Xm/omega_b*real(j*conj(Ias)*Iar);
Iqse = sqrt(2)*real(Ias);
Idse = -sqrt(2)*imag(Ias);
Iqre = sqrt(2)*real(Iar);
Idre = -sqrt(2)*imag(Iar);
psi_mqe = Xm*(Iqse+Iqre);
psi_mde = Xm*(Idse+Idre);
psi_qse = Iqse*Xls + psi_mqe;
psi_dse = Idse*Xls + psi_mde;
psi_qre = Iqre*Xlr + psi_mqe;
psi_dre = Idre*Xlr + psi_mde;
Te = psi_dse*Iqse - psi_qse*Idse;
psi_mqic=psi_mqe;
psi_mdic=psi_mde;
psi_qsic=psi_qse;
psi_dsic=psi_dse;
psi_qric=psi_qre;
psi_dric=psi_dre;
omegar_ic = omega_rotor;
end
```

LIST OF REFERENCES

[1] P. C. Krause, O. Wasynczuk, and S. D. Sudhoff, *Analysis of Electric Machinery and Drive Systems*, 2nd ed., John Wiley & Sons, 2002.

[2] A. Julian, Notes for EC 3130/EC 4130 (Advanced Electrical Machinery Systems), Naval Postgraduate School, Monterey, California, 2008 (unpublished).

[3] A. Julian, Induction Machine Model (Simulink/Matlab), March 2004.

[4] Roberto Cristi, *Modern Digital Signal Processing*, Thomson Brooks/Cole, 2004

[5] D. A. Andrade, A. W. F. V. Silveira, P. B. Severino, & T. S. Tavares, "DSP Based Torque Estimation in Three-phase Cage Induction Motor," *Electric Machines & Drives Conference*, vol. 2, May 2007, *IEEE* 1-4244-0743-5/07.

[6] D. Seyoum, D. McKinnon, M. F. Rahman, & D, Grantham, "Offset Compensation in the Estimation of Flux in Induction Machines," *Industrial Electronics Society*, vol. 2, November 2003, *IEEE* 0-7803-7906/03.

[7] Joseph E. O'Connor, "Field Programmable Gate Array Control of Power Systems in Graduate Student Laboratories," M.S. thesis, Naval Postgraduate School, Monterey, California, 2008.

THIS PAGE INTENTIONALLY LEFT BLANK

INITIAL DISTRIBUTION LIST

1. Defense Technical Information Center
   Ft. Belvoir, Virginia

2. Dudley Knox Library
   Naval Postgraduate School
   Monterey, California

3. Professor Alexander L. Julian
   Electrical and Computer Engineering Department
   Naval Postgraduate School
   Monterey, California

4. Professor Roberto Cristi
   Electrical and Computer Engineering Department
   Naval Postgraduate School
   Monterey, California

5. Professor Xiaoping Yun
   Electrical and Computer Engineering Department
   Naval Postgraduate School
   Monterey, California

6. Tsoutsas Athanasios
   Electrical and Computer Engineering Department
   Naval Postgraduate School
   Monterey, California